JOURNAL OF GEOPHYSICAL RESEARCH, VOL. 106, NO. C5, PAGES 9075–9092, MAY 15, 2001

River runoff, sea ice meltwater, and Pacific water distribution and mean residence times in the Arctic Ocean

Brenda Ekwurzel,[1] Peter Schlosser,[2,3] Richard A. Mortlock, and Richard G. Fairbanks[2]
Lamont-Doherty Earth Observatory of Columbia University, Palisades, New York

James H. Swift
Scripps Institution of Oceanography, University of California, San Diego, La Jolla, California

Abstract. Hydrographic and tracer data collected during ARK IV/3 (FS *Polarstern* in 1987), ARCTIC91 (IB *Oden*), and AOS94 (CCGS *Louis S. St-Laurent*) expeditions reveal the evolution of the near-surface waters in the Arctic Ocean during the late 1980s and early 1990s. Salinity, nutrients, dissolved oxygen, and $\delta^{18}O$ data are used to quantify the components of Arctic freshwater: river runoff, sea ice meltwater, and Pacific water. The calculated river runoff fractions suggest that in 1994 a large portion of water from the Pechora, Ob, Yenisey, Kotuy, and Lena Rivers did not flow off the shelf closest to their river deltas, but remained on the shelf and traveled via cyclonic circulation into the Laptev and East Siberian Seas. River runoff flowed off the shelf at the Lomonosov Ridge and most left the shelf at the Mendeleyev Ridge. ARCTIC91 and AOS94 Pacific water fraction estimates of Upper Halocline Water, the traditionally defined core of the Pacific water mass, document a decrease in extent compared to historical data. The front between Atlantic water and Pacific water shifted from the Lomonosov Ridge location in 1991 to the Mendeleyev Ridge in 1994. The relative age structure of the upper waters is described by using the ^3H-^3He age. The mean ^3H-^3He age measured in the halocline within the salinity surface of 33.1 ± 0.3 is 4.3 ± 1.7 years and that for the 34.2 ± 0.2 salinity surface is 9.6 ± 4.6 years. Lateral variations in the relative age structure within the halocline and Atlantic water support the well-known cyclonic boundary current circulation.

1. Introduction

One of the most important features of the Arctic Ocean is its well-developed halocline. The surface mixed layer and the highly stratified halocline form a low-salinity layer of water with temperatures close to the freezing point, which "blankets" a much thicker, more saline, and warmer layer of Atlantic origin. These low-salinity surface waters insulate the sea ice from the heat stored in the Atlantic water, which, if it were to reach the surface, could potentially melt or at least reduce the sea ice cover. Three freshwater sources maintain the halocline: river runoff, sea ice meltwater, and the low-salinity Pacific water entering the Arctic Ocean through the Bering Strait. The large storage of freshwater in the Arctic Ocean (around 100,000 km^3; [*Aagaard and Carmack*, 1989]) feeds freshwater outflows through Fram Strait and the Canadian Archipelago. *Blindheim et al.* [2000] link the winter North Atlantic Oscillation (NAO) index of wind forcing to reduced circulation of Atlantic water into the western Norwegian and Greenland Basins and increased circulation of upper layer Arctic water in the Norwegian Sea. Thus fluctuations in outflow of Arctic Ocean freshwater fractions combined with NAO atmospheric forcing will lead to variability in the rate and volume of convection in these regions.

Salinity has a profound influence on thermohaline circulation. The Arctic Ocean model results of *Häkkinen* [1993] support the hypothesis by *Aagaard and Carmack* [1989] that anomalously large ice export in 1968 caused a freshening of the northern North Atlantic known as the "Great Salinity Anomaly" (GSA) [*Dickson et al.*, 1988]. *Schlosser et al.* [1991] document a reduction during the 1980s of Greenland Sea Deep Water formation that may be linked to the return of the GSA to the Greenland Sea. *Steele and Boyd* [1998] demonstrated a significant decrease in the extent of the Cold Halocline Layer in the Eurasian Basin during the spring of 1995. In this context it is important to assess the volume, circulation pattern, and timescales for each of the freshwater components critical to maintaining properties of the Arctic Ocean mixed layer and halocline. The approach of our investigation is to quantify shifts in the Arctic Ocean freshwater components and check for possible links to proposed forcing mechanisms.

This study builds on previous work [*Schlosser et al.*, 1994; *Bauch et al.*, 1995; *Schlosser et al.*, 1995] by combining nutrients, dissolved oxygen, $\delta^{18}O$, tritium, and helium isotope data for determining the freshwater components and mean residence times of the upper waters in the Arctic Ocean. In this contribution, we use PO_4* (= PO_4^{3-} + O_2/175 -1.95 μmol kg^{-1} [*Broecker et al.*, 1985, 1998]) in combination with $\delta^{18}O$ and salinity to separate the Pacific water fraction from the river runoff

[1] Now at Department of Hydrology and Water Resources, University of Arizona, Tucson, Arizona.
[2] Also at Department of Earth and Environmental Sciences, Columbia University, New York.
[3] Also at Department of Earth and Environmental Engineering, Columbia University, New York.

Copyright 2001 by the American Geophysical Union

Paper number 1999JC000024.
0148-0227/01/1999JC000024$09.00

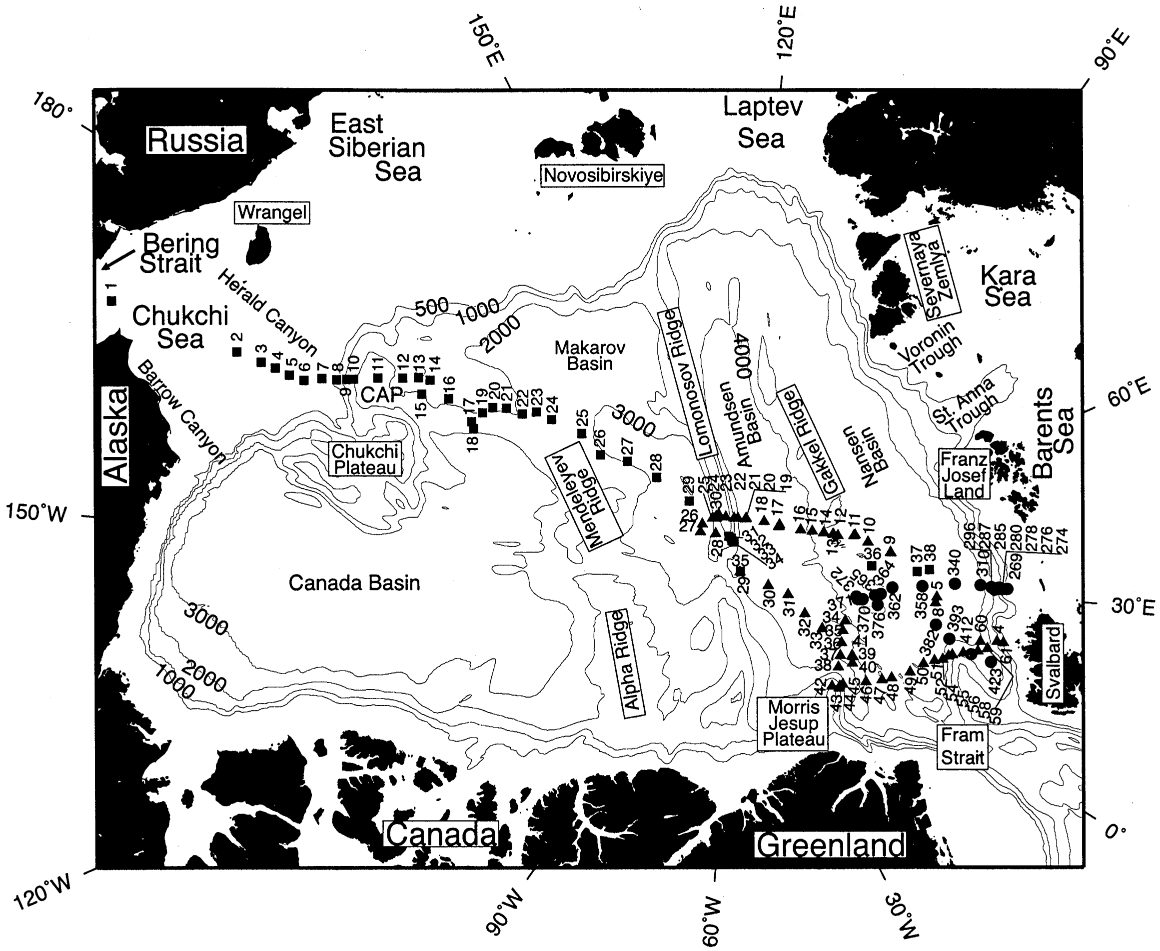

Figure 1. Station locations for ARK IV/3 (circle), ARCTIC91 (triangle), and AOS94 (square). CAP is an abbreviation for Chukchi Abyssal Plain.

and sea ice meltwater fractions contained in the Arctic freshwater. The residence times of the upper waters in the Arctic Ocean are determined from the ^{3}H-^{3}He age distribution.

2. Methods

2.1. Sample Collection

Salinity, nutrients, dissolved oxygen, $\delta^{18}O$, tritium, and helium samples were collected during icebreaker expeditions to the central Arctic Ocean. In summer 1987 the German icebreaker FS *Polarstern* crossed the Nansen Basin (ARK IV/3 expedition). The Swedish icebreaker IB *Oden* occupied Nansen, Amundsen, and a few Makarov Basin stations during the summer of 1991 (ARCTIC91 expedition). During the 1994 summer the Canadian icebreaker CCGS *Louis S. St-Laurent* crossed the southwestern boundary of the Canada Basin, surveyed the Makarov Basin, and occupied a few Eurasian Basin stations (AOS94 expedition). We collected water samples using a rosette system equipped with 10 L Niskin bottles during each cruise. The combined data set yields a comprehensive collection of tritium, helium, and $\delta^{18}O$ for the halocline waters over all basins between Fram Strait and Bering Strait (Figure 1).

2.2. Measurement

Temperature, salinity, oxygen, and nutrient samples were analyzed on each ship using techniques reported by *Anderson et al.* [1989, 1994], and *Swift et al.* [1997]. Tritium, helium isotopes, and some ^{18}O samples from ARK IV/3 were measured at the Institut für Umweltphysik at the University of Heidelberg following the methods described by *Roether* [1970] and *Bayer et al.* [1989]. All other tritium, helium isotopes, and ^{18}O samples were measured at the Lamont-Doherty Earth Observatory using procedures described by *Fairbanks* [1982] and *Ludin et al.* [1998]. Mass spectrometric measurements of the $H_2^{18}O/H_2^{16}O$ ratio were performed after water sample equilibration with CO_2 [*Epstein and Mayeda*, 1953; *Roether*, 1970; *Fairbanks*, 1982]. Oxygen isotope ratios are reported as $\delta^{18}O$ or the per mil deviation of the $H_2^{18}O/H_2^{16}O$ ratio of the sample from that of Standard Mean Ocean Water (SMOW) [*Craig*, 1961; *Gonfiantini*, 1981]. Measurement precision was about ±0.05-0.07‰ for a small portion of the ARK IV/3 $\delta^{18}O$ samples and about ±0.03‰ for the remaining $\delta^{18}O$ data.

Helium isotope ratios are reported as $\delta^{3}He$ or the percent deviation of the $^{3}He/^{4}He$ ratio of a measured sample from that of an air standard (R_{atm} = 1.386 x 10^{-6} [*Clarke et al.*, 1976]). Precision of the $^{3}He/^{4}He$ ratios was about ± 2‰. Tritium (^{3}H) has a half-life of 12.43 years [*Unterweger et al.*, 1980]. After sufficiently long storage (frozen at -25 °C) of the degassed water in flame-sealed glass bulbs, tritium values were determined by mass spectrometric measurement of the decay product ^{3}He. Tritium measurements had a precision of about ±2% and a detection limit of 0.03 TU, where 1 TU represents a tritium to hydrogen ratio of 10^{-18}. In order to compare data collected during different years all tritium data were decay-corrected to January 1, 1991, or TU91 units. This date is between the first and last cruise discussed in this study, and it follows the concept introduced by *Östlund and Hut* [1984], who report tritium data in TU81 units. The ^{3}H-^{3}He age or the time elapsed since the water left the surface is

$$\tau = \frac{1}{\lambda}\ln\left(1 + \frac{^3\mathrm{He_{tri}}}{^3\mathrm{H}}\right) \qquad (1)$$

where τ is the age (years), $^3He_{tri}$ is the tritiogenic ^{3}He concentration (TU), ^{3}H is the tritium concentration (TU), and λ is the ^{3}H decay constant.

3. Water Mass Definitions

Previous investigators have provided various classifications and names for portions of the water column surface, halocline, and Atlantic water (Figure 2). *Carmack* [1990] synthesizes the Arctic water mass definitions of *Swift and Aagaard* [1981] and *Aagaard et al.* [1985] in potential temperature Θ and salinity S space as follows: (1) Polar Water: near-freezing surface and main halocline water ($\Theta < 0$°C; $S < 34.4$); (2) Polar Intermediate Water, or arctic thermocline water: $\Theta < 0$°C; $34.4 < S < 34.7$; (3) Upper Arctic Intermediate Water: the core of the Atlantic layer in the Arctic Ocean ($\Theta < 2$°C; $34.7 < S < 34.9$); (4) Lower Arctic Intermediate Water ($0 < \Theta < 3$°C; $34.9 < S < 35.1$); and (5) Atlantic water: inflowing Norwegian-Atlantic current water ($\Theta >$ 3 °C; $S > 34.9$). The Atlantic water divides into two branches as it flows into the Arctic: (1) warm, saline water flows through Fram Strait known as the Fram Strait Branch Water (FSBW) and (2) water diverted onto the Barents shelf south of Svalbard cools and entrains shelf waters to become the colder and fresher Barents Sea Branch Water (BSBW) [*Schauer et al.*, 1997]. Recognizing the variable nature of the Atlantic inflow characteristics, shaded areas on Figure 2 are used to represent FSBW and BSBW instead of exact ranges.

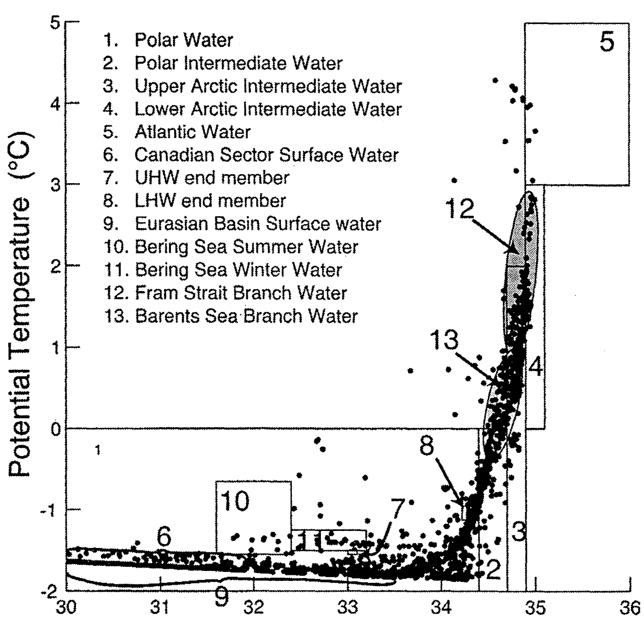

Figure 2. Selected water mass definitions, provided in the literature: 1-5 [*Carmack*, 1990]; 6-8 [*Jones and Anderson*, 1986]; 9 [*Coachman and Barnes*, 1962]; 10 and 11 [*Coachman and Barnes*, 1961]; and 12 and 13 [*Schauer et al.*, 1997]. The dots are bottle data for samples collected in the upper 300 m during ARK IV/3, ARCTIC91, and AOS94.

Coachman and Barnes [1961] find that the "Eurasian Basin Surface Water" has a wide range of salinities (28-33.5) and closely follows the freezing line. The Canadian Basin surface waters, however, exhibit temperature fluctuations with a local potential temperature maximum ($-1.55 < \Theta < -0.65$ °C at $31.6 < S < 32.4$) and a local Θ minimum ($-1.5 < \Theta < -1.25$ °C at $32.4 < S <$ 33.2). *Coachman and Barnes* [1962] call these "Summer Bering Sea Water" and "Winter Bering Sea Water," respectively. This classification implies not only the geographic location but also the season in which these water masses form.

Jones and Anderson [1986] noted the occurrence of a nutrient maximum and oxygen minimum near the 33.1 isohaline and referred to this water mass as "Upper Halocline Water" (UHW). They observed that a minimum in NO (NO = $9NO_3^- + O_2$ [*Broecker*, 1974]) occurred near a salinity of 34.2, which they defined as "Lower Halocline Water" (LHW). *Broecker* [1974] defines NO to account for the ratio of decomposition of organic matter in the nutrient balance and thereby identified a conservative tracer for water isolated from the atmosphere. *Rudels et al.* [1996] envision the formation of LHW with low NO as a stage in the evolution of inflowing Atlantic water as it travels into the Nansen Basin toward the Laptev Sea through a series of melt, freeze, and winter convection cycles. *Salmon and McRoy* [1994] suggest that the LHW advects into the Canada Basin where interleaving with shelf-derived water occurs, thereby increasing the nutrient content. They define this water as "Canada Lower Halocline Water." *McLaughlin et al.* [1996] recognized the difficulty with the traditional definitions and instead defined individual stations as belonging to a "Western Arctic Assembly," recognized by the presence of Pacific water, or an "Eastern Arctic Assembly," with no Pacific water. The terms UHW and LHW will be used in this contribution as a convenient way to differentiate the broad difference in these two parts of the Arctic Ocean halocline, while recognizing that each station represents a unique mixture of the above mentioned water masses.

4. Results and Discussion

4.1. Tracer $\delta^{18}O$

Fractionation between the heavier and lighter oxygen isotopes due to temperature and distance from the water vapor source area results in significant depletion of ^{18}O in Arctic runoff (relative to SMOW) and the Arctic Ocean into which these rivers flow (Figure 3). Hence $\delta^{18}O$ is a natural tracer of river runoff within the Arctic Ocean. Most of the samples in Figure 4 with salinities >34.1 fall along a mixing line between Atlantic water ($\delta^{18}O$: 0.3 ± 0.1 ‰) and Arctic river runoff (weighted average $\delta^{18}O$: -18‰; Figure 3). There is a sharp break at salinity 34.1-34.2 between higher-salinity waters falling on or above the Atlantic water-river mixing line and lower salinity waters falling below the mixing line. This break coincides with the salinity of LHW as defined by *Jones and Anderson* [1986]. Water samples with salinities <34.1 may also include waters of Pacific origin. The Pacific inflow through Bering Strait (Figure 4c) has a larger salinity range [*Roach et al.*, 1995] than the Atlantic inflow and has lower $\delta^{18}O$ values (~-1‰) because of the large influence of Alaskan and Siberian runoff to the Bering Sea [*Grebmeier et al.*, 1990; *Kipphut*, 1990; *Cooper et al.*, 1997]. Hence, for many samples, mixing is evident between Atlantic water, LHW, UHW, or Pacific inflow.

(a)

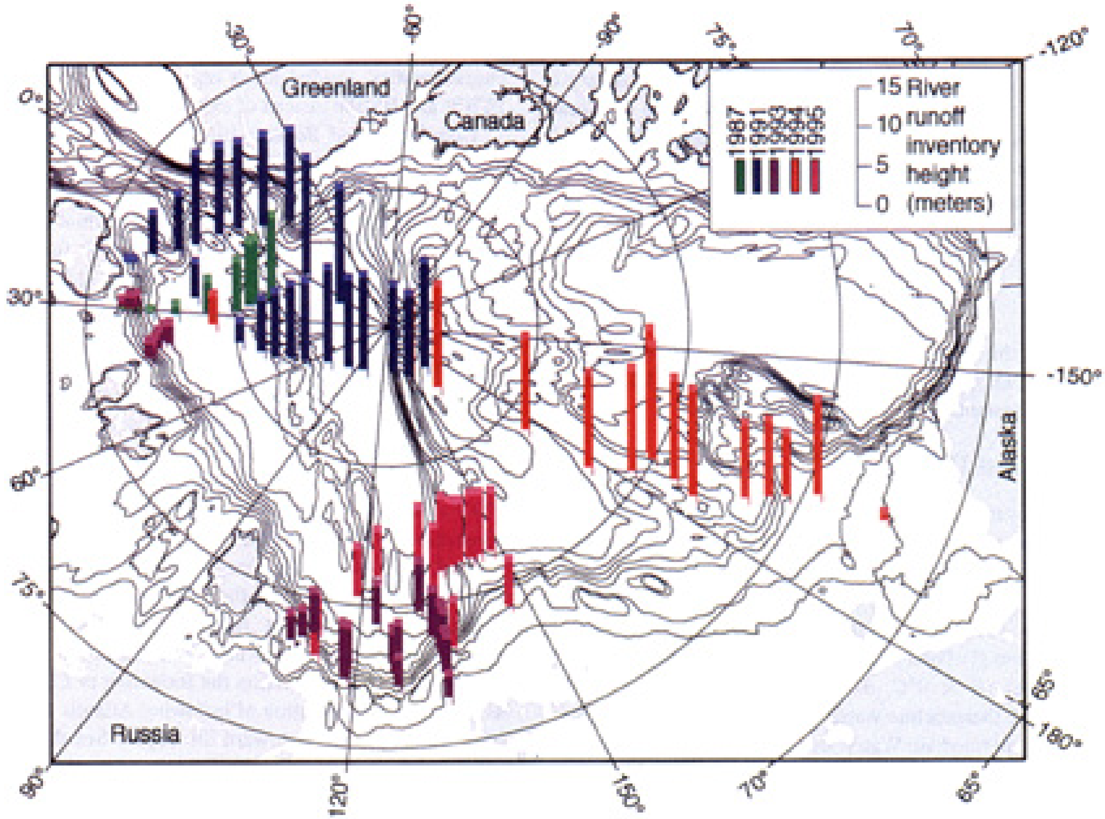

(b)

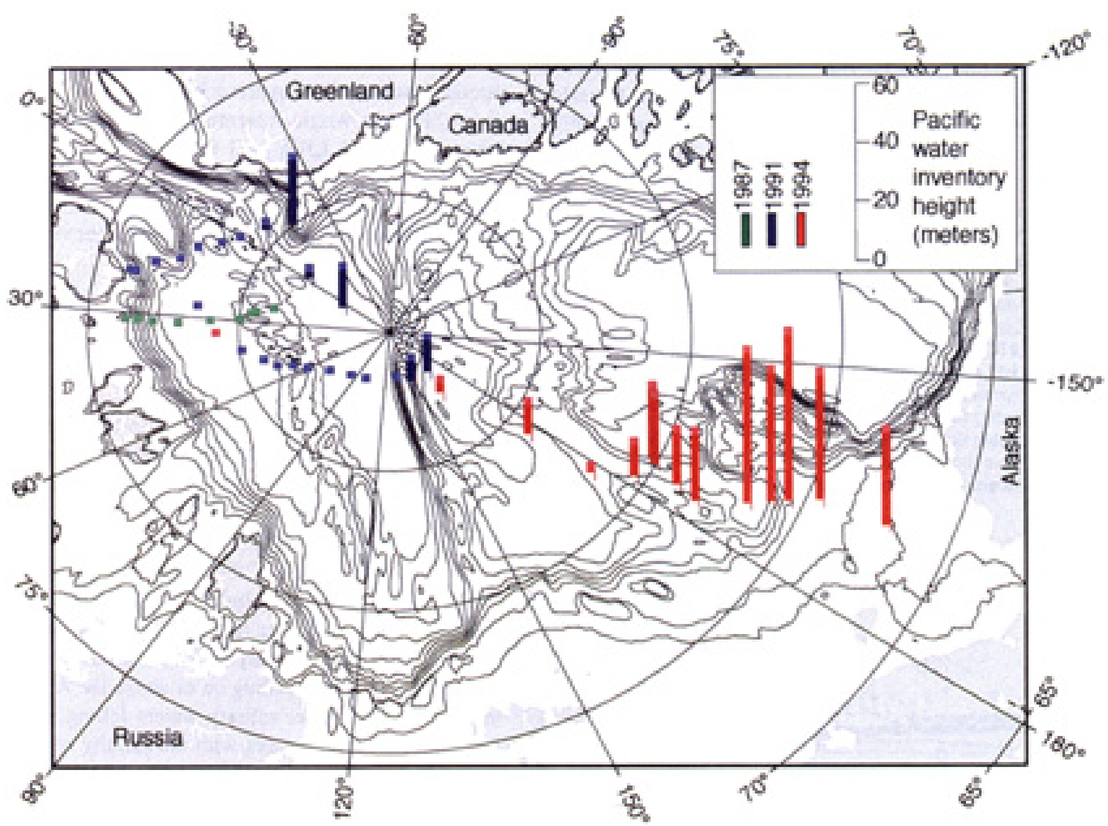

Plate 1. (a) River runoff water column inventory expressed as height in meters for the integrated water column between the surface and 300 m (or bottom measurement if shallower than 300 m) depth at each station. Also shown are the inventories *Frank* [1996] calculated for the 1993 ARK IX/4 and 1995 ARK XI/1 stations using a three-component mass balance with slightly different end-member concentrations. (b) Pacific water column inventory expressed as height in meters for the integrated water column between the surface and 300 m (or bottom measurement if shallower than 300 m) depth at each station.

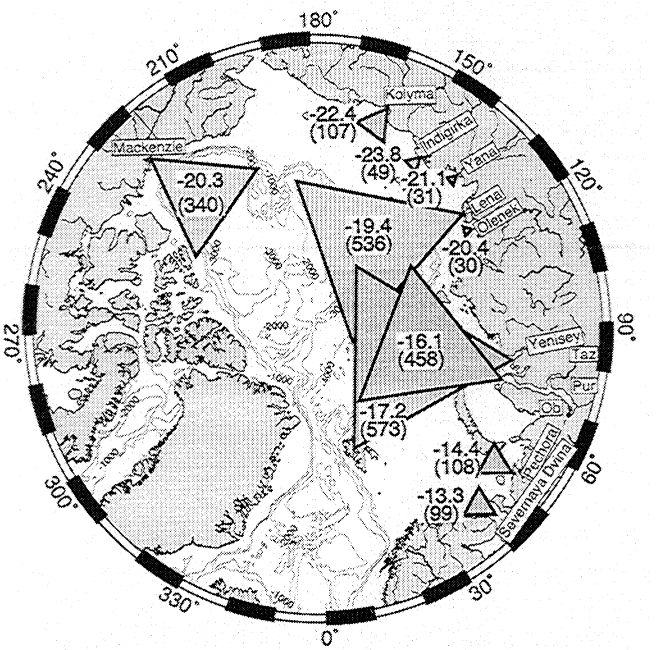

Figure 3. Mean annual discharge and $\delta^{18}O$ data available in the literature for Arctic Rivers. River discharge ($km^3\ yr^{-1}$) is proportional to triangle size and is listed in parenthesis within or near the triangle symbol for the river [*Becker*, 1995; *Pavlov et al.*, 1996]. The negative numbers within or near the triangle symbol for each river are the $\delta^{18}O$ (‰) values [*Macdonald et al.*, 1989; *Létolle et al.*, 1993; *Ekwurzel*, 1998].

Net sea ice melting and formation is another process recorded in the deviation of the samples from Atlantic water-river runoff mixing line in $\delta^{18}O$ versus salinity plots (see arrows of Figure 4). During sea ice formation, changes in salinity dominate. However, there is also a small enrichment of ^{18}O relative to the seawater from which it formed. The $\delta^{18}O$ equilibrium fractionation value (2.9‰) measured for freshwater ice in laboratory experiments [*Lehmann and Siegenthaler*, 1991] is higher than that measured by *Craig and Hom* [1968] (2.7‰) for sea ice formed from seawater under slow growth conditions. *Macdonald et al.* [1995] determined from Arctic field measurements the $\delta^{18}O$ fractionation of sea ice to be 2.6 ± 0.1‰, a value similar to the maximum equilibrium fractionation factor of 2.7‰ found by *Eicken* [1998] in the Weddell Sea. In the Beaufort Sea, *Melling and Moore* [1995] measured a mean fractionation factor of 2.1‰. *Eicken* [1998] stresses that rapid sea ice growth and different effective boundary layer thickness will produce a range of $\delta^{18}O$ fractionation factors. Conditions present in the Arctic could theoretically produce $\delta^{18}O$ fractionations between 1.5 and 2.7‰. Without knowing the exact dynamic fractionation factor we used 2.6‰ for our calculations, recognizing that the average may well be closer to that reported by *Melling and Moore* [1995]. Sensitivity tests [*Ekwurzel*, 1998] suggest that this uncertainty has little impact on the freshwater inventory calculations.

The sea ice fractionation effect can be seen in Figure 4a for the southern Nansen Basin (ARK IV/3 stations 269, 285, 287, and 310; ARCTIC91 stations 4, 8,9, and 61; and AOS94 station 37). These samples are the symbols that plot above the Atlantic water-river mixing line reflecting the addition of sea ice meltwater. Samples with salinities lower than that of the LHW have $\delta^{18}O$ values that reflect a combination of sea ice formation, mixing with river runoff, and, in many samples, mixing with a fraction of Pacific inflow waters.

4.2. PO_4^*

Nutrient-rich Pacific water flows through the shallow Bering Strait onto the Chukchi shelf where it is modified by a variety of shelf processes. Bering Strait freshwater inflow is estimated to be from one half of [*Aagaard and Carmack*, 1989] to equal to [*Becker*, 1995] the total Arctic river runoff. Pacific inflow therefore is a significant freshwater component of the Arctic surface and halocline waters, and its high level of nutrients is a key to calculating its fraction in the Arctic freshwater balance.

Cooper et al. [1997] hypothesize that the high-nutrient Bering Sea and Anadyr waters flowing through Bering Strait are depleted in nutrients on the Chukchi shelf during summer by biological growth or production and are not the waters that renew the nutrient maximum layer of the halocline known as UHW. However, during winter, as first suggested by *Coachman and Barnes* [1961] and confirmed by more recent studies [*Roach et al.*, 1995; *Cooper et al.*, 1997; *Weingartner et al.*, 1998], there

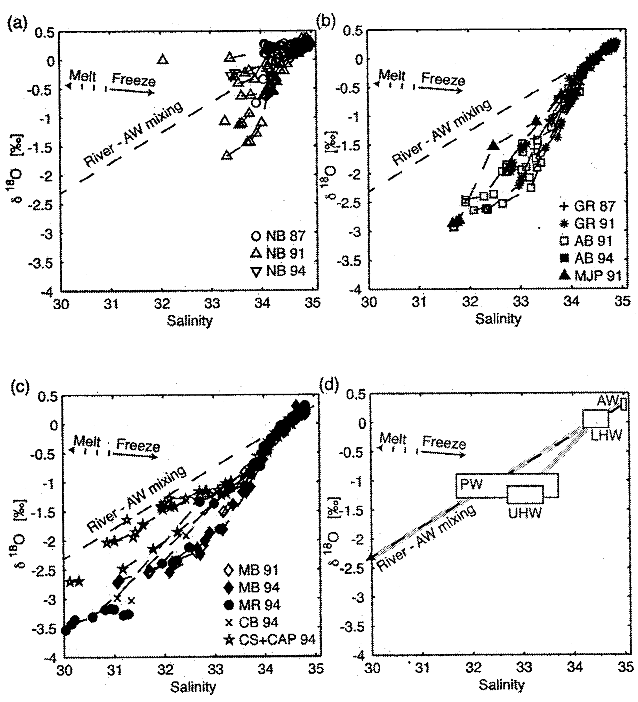

Figure 4. The $\delta^{18}O$ values versus salinity plots for stations from (a) Nansen Basin, (b) Gakkel Ridge and Amundsen Basin, (c) Canadian Basin, and (d) end members within the data range for Atlantic water, Pacific water, LHW, and UHW. Arrows indicate how ocean water concentration changes when water freezes to form sea ice or when sea ice melts. The dashed line represents mixing between Atlantic water and river water with -18‰ $\delta^{18}O$ concentration. Legend abbreviations are as follows: AB, Amundsen Basin; CAP, Chukchi Abyssal Plain; CB, Canada Basin; CS, Chukchi Sea; GR, Gakkel Ridge; MB, Makarov Basin; MJP, Morris Jesup Plateau; MR, Mendeleyev Ridge; NB, Nansen Basin; 87, ARK IV/3; 91, ARCTIC91; and 94, AOS94.

may be sufficient time for the nutrient-rich water to transit the shelf (i.e., when biological production is insignificant). In this scenario, winter transit is accompanied by a sufficient increase in salinity through brine rejection during sea ice formation to renew UHW (S ~ 33.1). These high-salinity shelf waters may be further enriched in nutrients by being in contact with shelf sediments that release nutrients from decay of organic matter [*Jones and Anderson*, 1986; *Anderson*, 1995]. Lower-salinity waters (S < 33.1) flowing through Bering Strait, predominantly Alaska Coastal Water, are more buoyant. They mix with Arctic river water and shelf waters influenced by sea ice meltwater and overlie the UHW [*Coachman et al.*, 1975].

Silicate has been used in previous studies to estimate the Pacific component contributing to the Arctic Ocean freshwater balance. However, Arctic rivers have a wide range of initial silicate concentrations (~25-160 μM kg^{-1} [*Macdonald et al.*, 1989; *Létolle et al.*, 1993; *Makkaveev and Stunzhas*, 1995; *Gordeev et al.*, 1996]) that are usually higher than the Pacific inflow concentration (~20 μM kg^{-1} [*Cooper et al.*, 1997]). Jones *et al.* [1998] also chose not to use silicate to trace Pacific water but instead used the nitrate-phosphate difference between Atlantic water and Pacific water end members to calculate Pacific water fraction in the upper 30 m.

Arctic rivers have phosphate concentrations close to zero [*Codispoti and Richards*, 1968; *Macdonald et al.*, 1987; *Makkaveev and Stunzhas*, 1995; *Gordeev et al.*, 1996]. In addition, Arctic river discharge occurs mainly during the summer months [*Becker*, 1995; *Pavlov et al.*, 1996; *Olsson*, 1997]; hence biological production during summer takes up most of the nutrients delivered to the Arctic Ocean by rivers [*Björk*, 1990]. Therefore we chose phosphate to estimate the contribution of the nutrient-rich Pacific inflow to the freshwater balance of the upper waters in the Arctic Ocean.

Recent refinement of the Redfield ratios [*Takahashi et al.*, 1985; *Anderson and Sarmiento*, 1994] are used to calculate PO_4* as a quasi-conservative water mass tracer that accounts for organic respiration [*Broecker et al.*, 1985, 1995]. The range between Atlantic water PO_4* (~0.7 μmol kg^{-1}) and Pacific water PO_4* (~2 μmol kg^{-1}) is significantly larger than individual measurement errors for PO_4^{3-} and O_2 [cf. *Swift et al.*, 1997, Table 1]. The one caveat is that Bering Strait inflow is variable and subject to seasonal processes mentioned above, and therefore the PO_4*, salinity, and $\delta^{18}O$ end member concentrations of Pacific water have higher uncertainties that create larger errors in the calculated freshwater fractions (see section 4.5 for a discussion the sensitivity tests regarding these end member uncertainties).

The PO_4* data are similar to $\delta^{18}O$ data in that they both highlight the mixing between Atlantic water and LHW at all stations. Almost all stations plotted in Figure 5 have their lowest PO_4* concentrations near the LHW salinity range, as expected from the low NO values of those waters [*Jones and Anderson*, 1986]. However, shelf stations in this data set often deviate from the general trend. Stations close to the Barents Sea shelf just north of Svalbard (ARCTIC91 stations 4, 60, and 61; open triangles outside the main cluster of data in Figure 5a) exhibit much lower PO_4* values. This may be the result of mixing with sea ice meltwater as indicated by the $\delta^{18}O$ trend for these samples (open triangles above the river-Atlantic water mixing line in Figure 4a). There is a slight elevation of PO_4* in the shelf stations sampled in 1987 (ARK IV/3 stations 269, 274, 276, and 278; open circles Figure 5a). This may reflect the influence of nutrient regeneration at the sediment water interface [*Anderson and Jones*, 1991] because these samples have a higher salinity

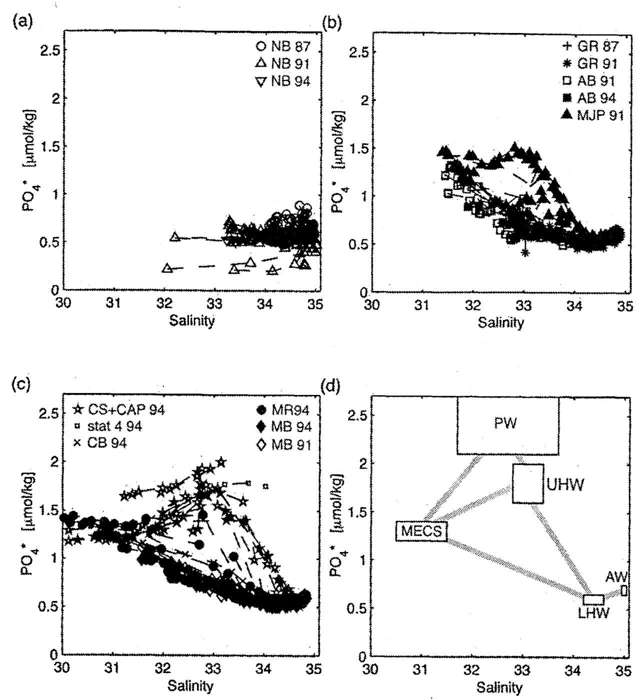

Figure 5. PO_4* versus salinity plots for stations from (a) Nansen Basin, (b) Gakkel Ridge and Amundsen Basin, (c) Canadian Basin, and (d) end members within the data range for Atlantic water, Pacific water, LHW, and UHW and Mixed East Siberian and Chukchi Shelf water (MECS). Legend abbreviations are explained in Figure 4.

than the Pacific inflow and are unlikely to have Pacific-derived water advected to this location [*Pfirman et al.*, 1997]. *Rey and Loeng* [1985] postulate regenerated nutrients to allow for the observed production during middle to late summer on the Barents Sea shelf. The remaining shelf stations in this data set are on the other side of the Arctic Ocean basin on the Chukchi shelf and have a wide range of salinities with high PO_4* values due to the dominance of Bering Strait inflow waters (star symbols, Figure 5c).

Nansen Basin and Amundsen Basin stations (excluding the more western stations sampled in 1991 between the Lomonosov Ridge and the Morris Jesup Plateau plotted as triangles on Figure 5b) fall along two mixing lines: (1) Atlantic water mixing with LHW and (2) LHW mixing with more buoyant (S < 33.2) surface waters with PO_4* values similar to those of the Atlantic water. Pacific water is not present in central and eastern Eurasian Basin waters sampled during this study.

Makarov Basin stations and Eurasian Basin stations located between the central Lomonosov Ridge and Morris Jesup Plateau extend the second mixing line of the above stations to fresher waters (S ~30.5-31.5) with higher PO_4* values (~1.4 μmol kg^{-1}), hereafter referred to as Mixed East Siberian and Chukchi Shelf water (MECS). Canada Basin stations near the Chukchi Abyssal Plain and Morris Jesup Plateau stations in the western Amundsen Basin group along three mixing lines: (1) Atlantic water mixing with LHW, (2) LHW mixing with Pacific water or UHW, and (3) Pacific water or UHW mixing with MECS.

The surface waters at the Morris Jesup Plateau (ARCTIC91 stations 40, 42, and 43; solid triangles that trace a high arch pattern in Figure 5b) contain Pacific water or UHW. Slightly away from the Morris Jesup Plateau (ARCTIC91 stations 37-39, 41, 44, and 45; solid triangles tracing a smaller arch pattern in Figure 5b), the surface waters follow the LHW-UHW mixing line for salinities between 32.8 and 34.2 and follow the LHW-MECS mixing line for fresher waters (S < 32.8). Several Mendeleyev Ridge stations (AOS94 stations12-18) are the solid circles plotting onto the smaller arch patterns in Figure 5c. The similarity between these Mendeleyev Ridge stations and the stations just offshore of the Morris Jesup Plateau supports the following connection or circulation pattern: buoyant fresh waters over the Mendeleyev Ridge reach to just offshore of the Morris Jesup Plateau.

Nutrient-rich Pacific water, most likely added by winter inflow, has salinities and temperatures sufficient for renewal of the halocline waters with salinities between 32.8 and 34.2. In the 1994 data these waters are limited to the Pacific side of the Mendeleyev Ridge. In contrast, the more buoyant components of Pacific inflow waters mix with river runoff and shelf waters to renew the freshest part of the halocline and are present over a larger portion of the Arctic Ocean (Canada Basin, central Makarov Basin, central Lomonosov Ridge, and western Amundsen Basin).

4.3. NO/PO

Aagaard et al. [1981] emphasize that the seasonal cycle of summer melt and winter sea ice formation on the shelf seas is an important process for creating a thick Arctic Ocean halocline. If we can identify where shelf regions currently renew halocline waters, we may be able to use this information to model how the halocline will respond to changes in winter sea ice formation rates under different phases of the Arctic Oscillation.

Wilson and Wallace [1990] found that Arctic shelf waters have regionally distinctive NO/PO ratios. They used the Redfield ratios of *Broecker* [1974] in their definition of NO ($9NO_3^- + O_2$) and PO ($135PO_4^{3-} + O_2$) instead of the revised Redfield ratio by *Broecker et al.* [1985] ($175PO_4^{3-} + O_2$). The NO/PO ratio used in this study is the ratio by *Wilson and Wallace* [1990], hereinafter referred to as ($NO/PO_{(135)}$), to be consistent with their values defined for the shelf waters (Figure 6). Kara Sea data were not available for their study, and therefore ratios were defined only for the Barents Sea shelf, the Laptev Sea shelf, the East Siberian Sea shelf, and the Chukchi Sea shelf.

Cooling and freshening of Atlantic water (both the FSBW and BSBW) on its transit to the eastern Eurasian Basin have been proposed as the first steps toward forming LHW [*Jones and Anderson*, 1986; *Steele et al.*, 1995; *Rudels et al.*, 1996]. The stations sampled for this study support the above hypothesis because waters with salinities greater than those of LHW all fall within the Barents Sea $NO/PO_{(135)}$ range (Figure 6). The exceptions to this trend are the lower $NO/PO_{(135)}$ ratios of the Chukchi Abyssal Plain samples with salinities >34.2. *Salmon and McRoy* [1994] and *McLaughlin et al.* [1996] found similar trends for other Canada Basin stations. The Chukchi Abyssal Plain stations (star symbols on Figure 6c) and Morris Jesup Plateau stations (solid triangles on Figure 6b) exhibit mixing between Atlantic water-LHW and UHW with salinities around 32.8-33.1, which are overlain by waters falling on the mixing line with Chukchi Sea shelf waters.

The freshest Nansen Basin, Gakkel Ridge, and central Amundsen Basin halocline waters are within the Barents Sea $NO/PO_{(135)}$ range. The Lomonosov Ridge stations range between the Barents Sea and the lower limit of the Laptev Sea $NO/PO_{(135)}$ ratios. This is consistent with the capping of LHW by Laptev Sea shelf waters proposed by *Rudels et al.* [1996] and the direction of the Transpolar Drift [*Thorndike and Colony*, 1982; *Pfirman et al.*, 1997]. The Makarov Basin and western Amundsen Basin stations contain a mixture between higher-salinity Barents Sea and Laptev Sea $NO/PO_{(135)}$ ratios and the lower-salinity waters at the boundary between the $NO/PO_{(135)}$ ratios of East Siberian Sea and Chukchi Sea shelf waters. $NO/PO_{(135)}$ ratios in Chukchi Abyssal Plain surface waters point toward a Chukchi Sea source, while those in Mendeleyev Ridge surface waters point toward an East Siberian Sea source. Hence the stations mark an increased progression of shelf inputs from the Barents Sea, Kara Sea, Laptev Sea, East Siberian Sea, and Chukchi Sea into the freshest part of the Arctic halocline.

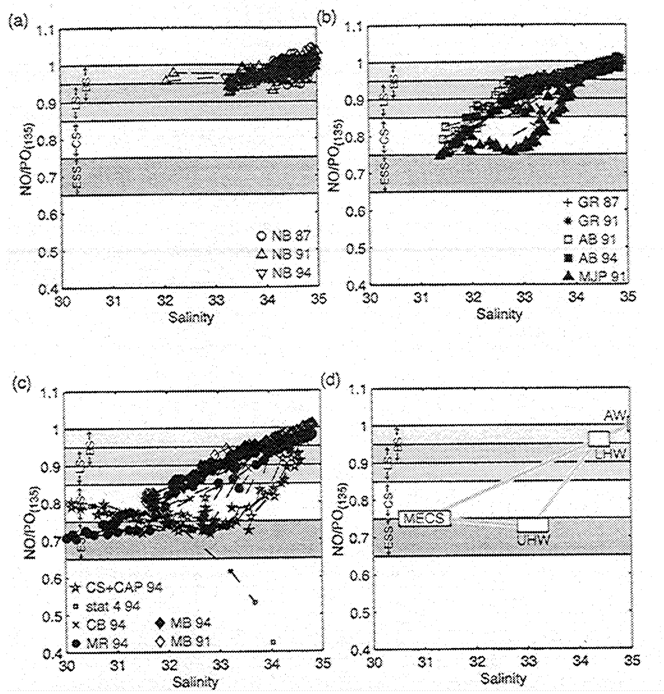

Figure 6. $NO/PO_{(135)}$ versus salinity plots for stations from (a) Nansen Basin, (b) Gakkel Ridge and Amundsen Basin, (c) Canadian Basin, and (d) end members within the data range for Atlantic water, Pacific water, LHW, and UHW and MECS. Boxes in each graph are the ranges of *Wilson and Wallace* [1990]. BS is Barents Sea, LS is Laptev Sea, CS is Chukchi Sea, ESS is East Siberian Sea, and legend abbreviations are explained in Figure 4. AOS94 station 4 in Figure 6c falls below established $NO/PO_{(135)}$ ratios. It represents a pool of high-salinity Chukchi shelf water with the highest phosphate and silicate as well as the lowest oxygen values recorded in this data set.

4.4. End-Member Characteristics

The mixing relationships outlined above imply an intricate interaction between the freshwater components of the surface and halocline waters. Each geochemical tracer highlights specific freshwater components in a different way. For example, high PO_4* levels emphasize the Pacific influence, but it would be difficult to assess the river runoff factor from PO_4* alone. Combining salinity, $\delta^{18}O$, and PO_4* allows for a quantitative determination to these freshwater fractions in each sample where all three measurements exist.

Östlund and Hut [1984] first proposed combining δ^{18}O and salinity measurements to separate the river runoff from the sea ice meltwater contribution to the Atlantic derived water. This method was successfully employed on the Mackenzie shelf in the Beaufort Sea [*Macdonald and Carmack*, 1991; *Macdonald et al.*, 1995; *Melling and Moore*, 1995] and in the Eurasian Basin [*Schlosser et al.*, 1994; *Bauch et al.*, 1995; *Frank*, 1996]. We extend the oxygen isotope data into the eastern Eurasian Basin and Canadian Basin and recalculate the ARK IV/3 and ARCTIC91 data presented by *Bauch et al.* [1995], adding PO_4* as a fourth component to isolate the Pacific fraction.

The four-component mass balance equations are as follows:

$$f_a + f_p + f_r + f_i = 1, \tag{2}$$

$$f_a S_a + f_p S_p + f_r S_r + f_i S_i = S_m, \tag{3}$$

$$f_a \delta^{18}O_a + f_p \delta^{18}O_p + f_r \delta^{18}O_r + f_i \delta^{18}O_i = \delta^{18}O_m, \tag{4}$$

$$f_a PO_4{}^*{}_a + f_p PO_4{}^*{}_p + f_r PO_4{}^*{}_r + f_i PO_4{}^*{}_i = PO_4{}^*{}_m, \tag{5}$$

where f_a, f_r, f_i, f_p are the fractions of Atlantic water, river runoff, sea ice meltwater, and Pacific water contributing to a measured water sample (subscript *m*) and S_x, $\delta^{18}O_x$, and $PO_4{}^*{}_x$ are the corresponding salinity, δ^{18}O, and PO_4* water mass concentrations. The fractions f_x are also used to calculate the volume of water attributable to each freshwater component. At each station the fractions were linearly interpolated to a depth of 300 m (or to the deepest depth if shallower than 300 m) and extrapolated to the surface. This interpolated profile was integrated by trapezoidal approximation to yield a total height in meters (termed the inventory height) as a proxy for volume.

Not all the waters in the Arctic Ocean halocline have a Pacific-derived component. The four-component mass balance calculations were run on all samples to determine which waters contain a Pacific component. If the four-component solution of a sample results in a negative f_p value, then Pacific water was not present. In this case we used the salinity and δ^{18}O data and solved the three-component mass balance equations (i.e., equations (1), (2), and (3) without the f_p, $f_p S_p$, and $f_p \delta^{18}O_p$ variables).

To prepare for the mass balance calculation, a representative tracer concentration must be determined for each water mass before it enters the Arctic Ocean (i.e., Fram Strait, Bering Strait, river mouth, and sea ice at the surface). Using a single-tracer concentration for each end member averages over the natural variability of the system. For example, each river does not have the exact same δ^{18}O value (Figure 3). Sensitivity tests for the central Arctic Ocean data reveal that the uncertainty in the range of each end-member concentration does not significantly affect the first order results obtained by the mean end-member values (see section 4.5).

The Atlantic water salinity (Table1) is well constrained and is based on the Meteor 8 section between Norway and Svalbard on the Barents Sea shelf and the *Polarstern* ARK IX/1 Fram Strait section at 79°N [*Frank*, 1996]. Initial sea ice salinity can have a wide range ($5 < S < 12$), but multiyear ice has a salinity with a mean value of 4 ± 1 [*Untersteiner*, 1968; *Pfirman et al.*, 1990; *Melling and Moore*, 1995; *Melnikov*, 1997]. The Pacific salinity end-member concentration has been set to 32.7 ± 1 [*Roach et al.*, 1995].

Table 1. Parameters Used in Three-Component and Four-Component Mass Balance

	Salinity	δ^{18}O, ‰	PO_4*, μmol kg^{-1}
Atlantic water	35 ± 0.05	0.3 ± 0.1	0.7 ± 0.05
River runoff	0	-18 ± 2	0.1 ± 0.1
Sea ice	4 ± 1	surface + (2.6 ± 0.1)[a]	0.4 ± 0.2
Pacific water	32.7 ± 1	-1.1 ± 0.2	2.4 ± 0.3

[a]For each station this value is set as the surface δ^{18}O measurement plus the equilibrium fractionation factor [*Macdonald et al.*, 1995; *Eicken*, 1998] during sea ice formation [*Östlund and Hut*, 1984].

The Atlantic δ^{18}O value (0.3 ± 0.1‰) originally determined by *Östlund and Hut* [1984] is supported by Meteor 8 Barents Sea shelf and ARK IX/1 Fram Strait sections [*Frank*, 1996], and by Atlantic water measurements from ARK IV/3 [*Schlosser et al.*, 1994], ARCTIC91 [*Bauch et al.*, 1995], and AOS94 stations. The river end-member δ^{18}O concentration (-18‰) is based on the river δ^{18}O measurements weighted by their respective discharge values (Figure 3)

The question remains if the above weighted mean is representative when we do not currently have δ^{18}O data from smaller rivers and when we are accounting for contribution from high-latitude precipitation. To address this concern, we consulted the Global Network for Isotopes in Precipitation (GNIP) database of the International Atomic Energy Agency (IAEA, http://www.iaea.org/programs/ri/gnip/gnipmain.htm, 1998). All GNIP stations at latitudes >65°N are listed in Table 2. As with the river data, the general trend is toward more depleted δ^{18}O in precipitation the farther east the station is located on a 360° scale. The average for these precipitation data is -19.9‰ δ^{18}O, and for stations with monthly rainfall measurements the weighted average is -18.1‰ δ^{18}O. If we were focusing on determining a more precise river runoff fraction for a shelf sea, we could use the δ^{18}O end member specific to that shelf area. However, for the central Arctic Ocean, where all the river sources are mixed together, one end member is chosen, and sensitivity tests for the effect of the uncertainty in each end member serve as a guide to our interpretations.

Following the method first outlined by *Östlund and Hut* [1984], the sea ice δ^{18}O values were calculated for each station as the surface water δ^{18}O measurement plus the maximum equilibrium fractionation factor of 2.6 ± 0.1‰ [*Macdonald et al.*, 1995; *Eicken*, 1998]. The Bering Strait data by *Cooper et al.* [1997] are used for the Pacific δ^{18}O end-member value (-1.1 ± 0.2‰).

The Atlantic PO_4* end-member concentration is based on PO_4* data reported by *Broecker et al.* [1995] and the Atlantic water data at ARK IV/3 and ARCTIC91 stations close to Fram Strait. The PO_4* concentration for river runoff was calculated from phosphate and oxygen data from the Ob and Yenisey Rivers [*Makkaveev and Stunzhas*, 1995] and Mackenzie River phosphate data [*Macdonald et al.*, 1987]. The Mackenzie River phosphate-salinity relationship implies a net loss of phosphate in the estuary possibly due to particle scavenging.

Extensive sea ice phosphate measurements were performed for all seasons during the drifts of the Arctic and Antarctic Research Institute "North Pole" ice stations NP-22 and NP-23. *Melnikov* [1997] reports a seasonal decrease (June to November) of phosphate concentrations as the ice algae utilize the nutrients

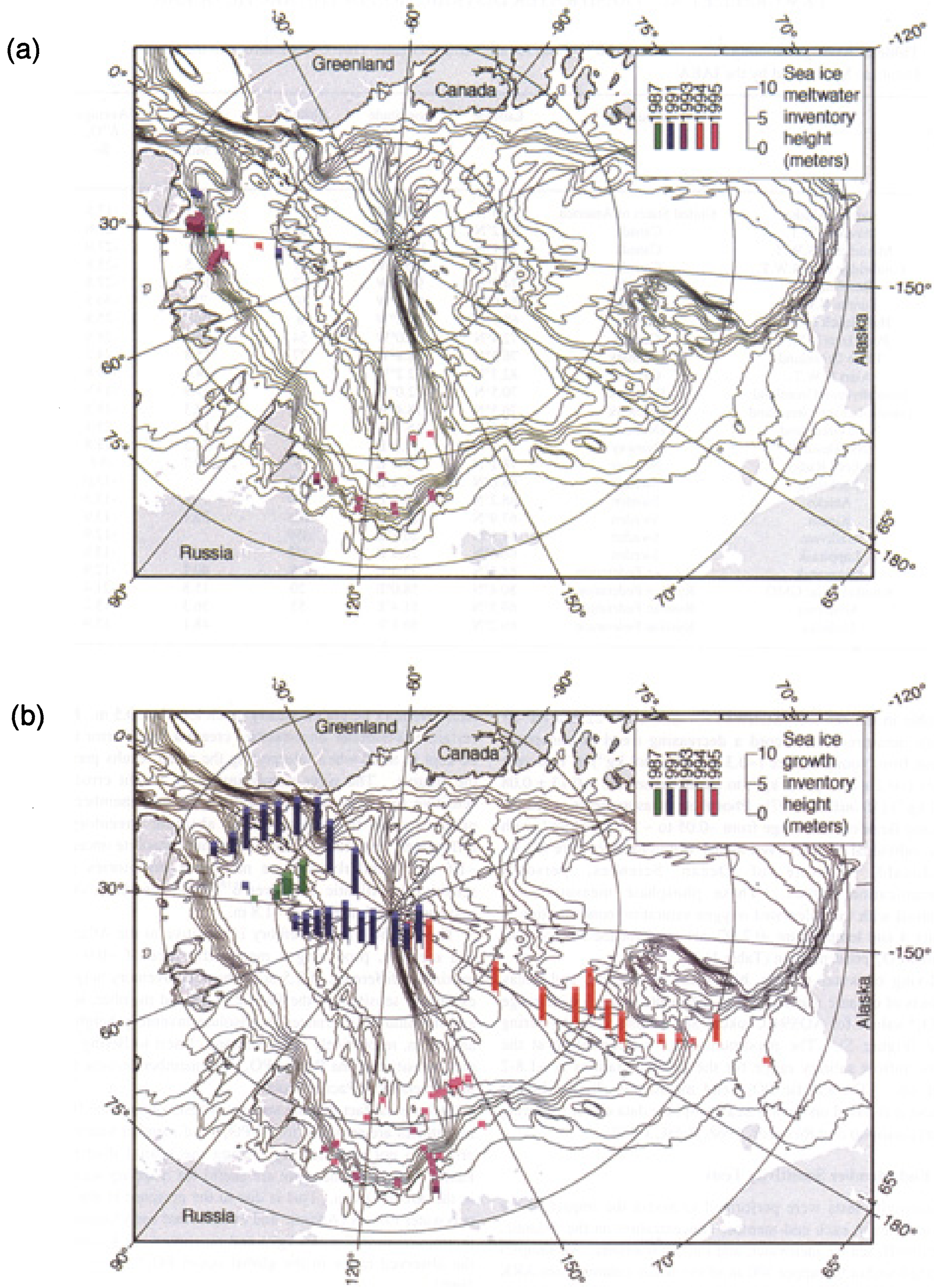

Plate 2. Net sea ice meltwater water column inventory expressed as height in meters for the integrated water column between the surface and 300 m (or bottom measurement if shallower than 300 m) depth at each station. (a) Positive numbers are net sea ice meltwater addition and (b) negative numbers represent net freshwater removed to form sea ice but are depicted here as positive bar heights. Also shown are the inventories *Frank* [1996] calculated for the 1993 ARK IX/4 and 1995 ARK XI/1 stations using a three-component mass balance with slightly different end-member concentrations.

Table2. Average Monthly Precipitation and $\delta^{18}O$ Data for all Stations Greater Than 65°N Latitude in the GNIP Database Maintained by the IAEA

Station	Country	Latitude	Longitude	Altitude, m	Average Precipitation per Month, mm	Average $\delta^{18}O$, ‰
Barrow Alaska	United States of America	71.3°N	156.8°W	7	11.1	-17.8
Inuvik N.W.T.	Canada	68.2°N	133.3°W	68	16.2	-27.6
Mould Bay N.W.T.	Canada	76.1°N	119.2°W	15	9.9	-27.0
Cambridge Bay N.W.T.	Canada	69.1°N	105.1°W	27	11.5	-25.8
Resolute Bay	Canada	74.7°N	95.0°W	67	10.9	-27.8
Eureka N.W.T.	Canada	80.0°N	85.6°W	10	7.0	-30.5
Hall Beach N.W.T.	Canada	68.5°N	81.2°W	8	14.8	-25.8
Pond Inlet N.W.T.	Canada	72.4°N	78.0°W	54	16.1	-28.9
Thule Greenland	Denmark	76.5°N	68.8°W	77	15.8	-24.2
Alert N.W.T.	Canada	82.3°N	62.2°W	62	14.0	-30.8
Scoresbysund Greenland	Denmark	70.5°N	22.0°W		37.9	-13.8
Danmarkshavn Greenland	Denmark	76.5°N	18.4°W	12	18.3	-18.5
Nord Greenland	Denmark	81.6°N	16.7°W	35	14.4	-25.1
Ny Alesund	Norway	78.2°N	11.9°E	7	34.5	-11.8
Isfjord Radio	Norway	78.1°N	13.6°E	6	40.7	-9.6
Racksund	Sweden	66.0°N	17.4°E	432		-13.0
Abisko	Sweden	68.2°N	18.5°E	392		-13.3
Kiruna	Sweden	67.9°N	20.2°E	505	32.7	-13.9
Gallivare	Sweden	67.1°N	20.3°E	359		-12.9
Lapptrask	Sweden	66.3°N	22.3°E	252		-13.9
Murmansk	Russian Federation	68.6°N	33.0°E	46	40.2	-12.9
Krenkel Polar GMO	Russian Federation	80.4°N	58.0°E	20	15.8	-21.4
Amderma	Russian Federation	69.5°N	61.4°E	53	36.3	-15.7
Dudinka	Russian Federation	69.2°N	86.1°E		48.1	-15.9

available in the sea ice. Statistics for all the NP-22 and NP-23 sea ice measurements record a decreasing trend in phosphate content from young sea ice (~0.3 ± 0.07 μmol kg^{-1}) to first-year sea ice (~0.2 ± 0.15 μmol kg^{-1}) to multiyear sea ice (~0.13 ± 0.08 μmol kg^{-1}) [*Melnikov*, 1997]. Phosphate measurements in sea ice from the Beaufort Sea range from ~0.05 to ~ 0.6 μmol kg^{-1}, with a few individual samples even higher within each ice core (R. W. Macdonald, Institute of Ocean Sciences, personal communication, 1998). These phosphate measurements, combined with the calculated oxygen saturation concentration at salinity 4 and temperature -0.2 °C, are used for the sea ice end-member PO_4*concentration (Table 1).

Mixing of water masses, biological production, and decay products of organic material in the sediments create a wide range of PO_4* values for AOS94 Chukchi Sea stations close to Bering Strait (Figure 5). The maximum PO_4* concentration at the Pacific inflow salinity range for the AOS94 stations is ~1.8-2 μmol kg^{-1}. The Pacific PO_4* end member is slightly higher because it is based on Bering Sea phosphate data closer to Bering Strait [*Codispoti and Richards*, 1968; *Björk*, 1990].

4.5. End-Member Sensitivity Tests

Sensitivity tests were performed to assess the impact of the uncertainties in each end-member concentration on the Atlantic, river runoff, sea ice meltwater, and Pacific fractions. All samples collected within the upper 300 m of the water column from ARK IV/3, ARCTIC91, AOS94, and ARK XII/1 (a 1996 expedition not reported in this contribution) were calculated using the mean end-member concentrations listed in Table 1. These results were then compared to calculations where one end-member concentration was changed at a time to the maximum error value (see *Ekwurzel* [1998] for details). Uncertainties cause an error in total inventory height of usually much less than 0.5 m. However, certain end-member uncertainties create a larger error that must be kept in mind when interpreting the mean results presented in the figures. The river runoff inventory height error is most sensitive to the river and Atlantic $\delta^{18}O$ end members, which produce ~0.8 to ~1.4 m mean absolute inventory height differences, respectively, and a maximum absolute uncertainty of ~1.6 m. Similarly, sea ice meltwater inventories are most sensitive to Atlantic and river $\delta^{18}O$ end members, creating a maximum absolute error of ~1.8 m.

The Pacific water inventory is sensitive to the Atlantic PO_4* end member, producing a mean difference of ~0.9 m and a maximum difference of 2.5 m in absolute inventory height, and is extremely sensitive to the Pacific PO_4* end member, with mean and maximum differences in absolute inventory height of ~2.4 and 12 m, respectively. The stations closest to Bering Strait are most sensitive to the Pacific PO_4* end member because they have high fractions of Pacific water.

Despite the fact that the sensitivity tests suggest the freshwater inventories are sensitive to the PO_4* end-member uncertainty the errors do not significantly change the spatial distribution of Pacific water and therefore are useful for mapping water masses in the Arctic Ocean. This is due to the presence in the Arctic of two water masses (Atlantic and Pacific) that carry signals close to the minimum (0.7 μmol kg^{-1}) and maximum (2.4 μmol kg^{-1}) of the observed range in the global ocean PO_4* [*Broecker et al.*, 1998].

4.6. Sea Ice

Predominant freshwater circulation patterns can be inferred from (1) solutions of the mass balance equations presented along a series of sections from 0 to 300 m depth between the Barents

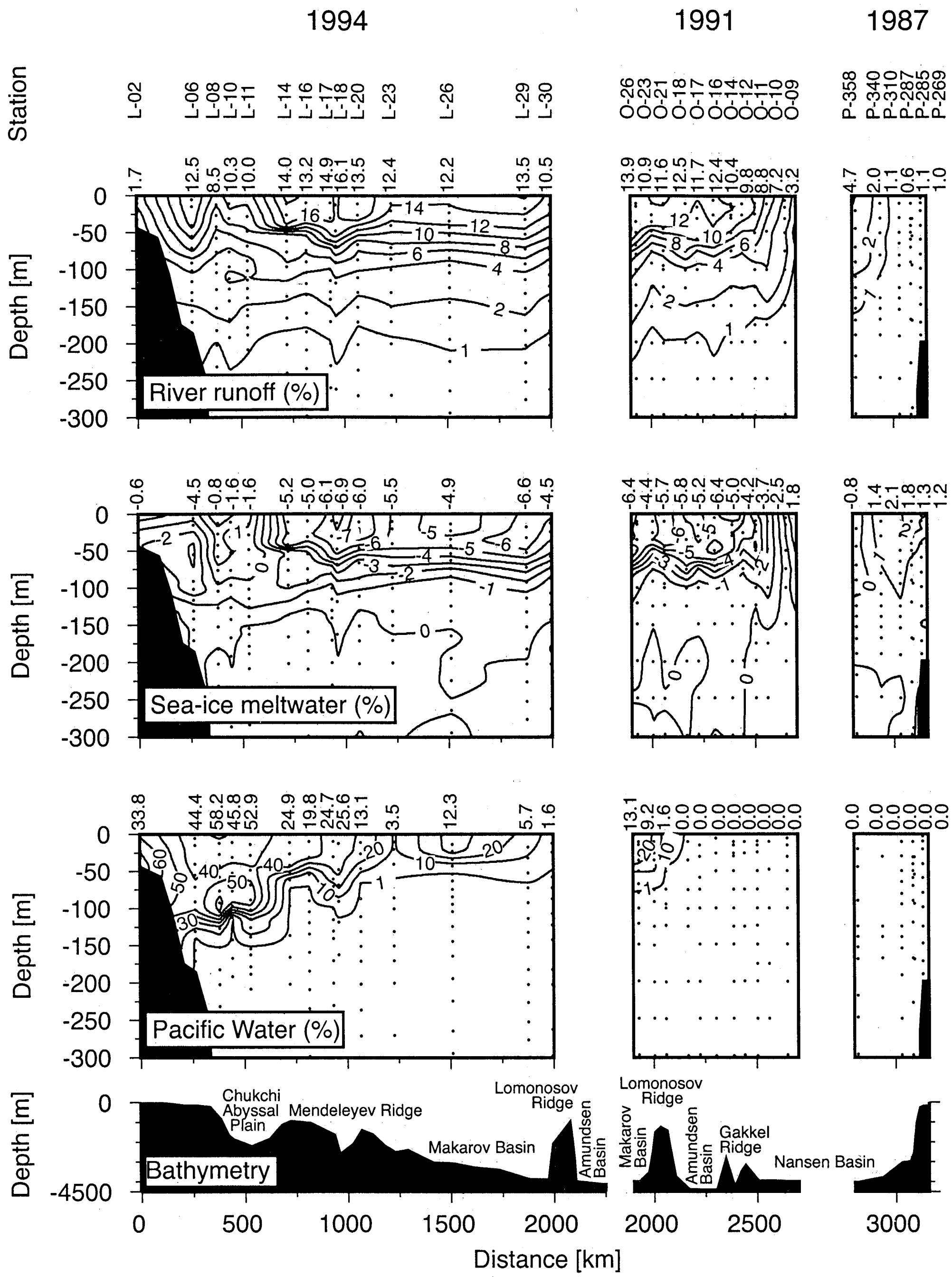

Figure 7. River runoff, sea-ice meltwater, and Pacific water fraction distribution in the upper 300 m water column along several sections spaced over several years and three expeditions between the Chukchi shelf north of Bering Strait and the Barents shelf north of Svalbard. The year of each expedition is located at the top of the sections and the station number codes are P, *Polarstern* (ARK IV/3); O, *Oden* (ARCTIC91); and L, *Louis S. St-Laurent* (AOS94). Figure 1 depicts the location of each station. Numbers above each station in each section are the station inventory expressed as height in meters for the integrated water column between the surface and 300 m (or bottom measurement if shallower than 300 m) depth at each station. For the sea ice meltwater sections, positive numbers reflect freshwater addition by sea ice melting and negative numbers represent freshwater removal during sea ice formation.

Shelf north of Svalbard and the Chukchi Sea (Figure 7) and (2) maps of total freshwater fraction inventories for each station (Plates 1 and 2). The sections do not represent a synoptic view because there were significant property shifts in the Arctic surface and halocline during the early 1990s. Indeed, these series of sections serve to highlight some of these changes, particularly over the Lomonosov Ridge where there is geographic overlap.

Following the interpretation of *Östlund and Hut* [1984], negative sea ice fractions and inventories represent the portion of freshwater used to form sea ice, whereas positive values indicate freshwater generated by sea ice melting. Southern Nansen Basin surface and halocline waters sampled in 1987 and 1991 are formed from inflowing Atlantic water and sea ice meltwater, consistent with halocline water formation processes described by

Steele et al. [1995] and *Rudels et al.* [1996]. The near-surface waters observed in this region contain as much as 2% of sea ice meltwater, <1% of river runoff, and no Pacific water (Figure 7). A narrow region (~200 km) containing sea ice meltwater immediately north of Svalbard widens to ~500 km farther east between Svalbard and Franz Joseph Land (Plate 2). This may reflect the different influence of the Fram Strait Branch of Atlantic water and Barents Sea shelf water on the surface mixed layer and halocline formation [*Pfirman et al.*, 1994; *Schauer et al.*, 1997]. Net sea ice melting extends to the shelf slope near Severnaya Zemlya, where 1993 (ARK IX/4) sea ice meltwater inventories remain in excess of 1 m [*Frank*, 1996]. The 1993 ARK IX/4 data in the Nansen Basin at the Laptev Sea shelf break show mostly positive sea ice meltwater inventories just offshore of the shelf break.

In 1987 and 1991 a sharp front exists in the Nansen Basin, where we observe a shift in surface and halocline source waters from net sea ice melting to net sea ice formation, a river runoff increase, and the absence of Pacific water (Plates 1 and 2). ARCTIC91 station 58, ARK IV/3 station 358, and ARCTIC91 station 10 trace this front.

4.7. River Runoff

The most striking feature of the mass balance solutions is the high river runoff fractions (>14%) in the upper 50 m over the Mendeleyev Ridge (AOS94 stations 14, 16, 17, 18, and 20 in Figure 7). The $NO/PO_{(135)}$ ratio for the Mendeleyev Ridge surface waters points to an East Siberian Sea source area (Figure 6). Dissolved barium concentrations suggest Mackenzie River water may also be present over the Mendeleyev Ridge [*Guay and Falkner*, 1997]. Hence in 1994 the dominant location for mixing of river runoff that has left the Siberian shelf is the Mendeleyev Ridge.

On the Chukchi shelf slope we observed higher upper water column river runoff percentages than in the adjacent shelf waters or in waters seaward of the shelf break (Figure 7). AOS94 station 6 located over the Chukchi Sea shelf slope has higher river runoff fractions (>10% in the upper 50 m) than does Chukchi Sea shelf station 2 (>2%) and Chukchi Abyssal Plain stations 8, 10, and 11 (>6% in the upper 50 m). This suggests strong topographic steering of river runoff flow after it has left the shelf break.

Three component mass balance calculations for the 1995 Kara Sea and 1992, 1993, and 1995 Laptev Sea demonstrate that the high river runoff fractions on the shelf decrease dramatically seaward of the shelf break [*Bauch*, 1995; *Frank*, 1996]. In contrast, the upper 50 m of the Makarov Basin along the AOS94 section contained more than 10% river runoff. These combined river runoff fraction results suggest that during the early 1990s a significant portion of Pechora, Ob, Yenisey, Kotuy, and Lena river waters did not flow off the shelf closest to their river deltas. Instead, they remained mostly on the shelf, circulating cyclonically into the East Siberian Sea, where most of the river runoff moved off the shelf along the Mendeleyev Ridge and Chukchi Plateau.

Furthermore, the river runoff inventory distribution (Plate 1) in combination with the $NO/PO_{(135)}$ results (Figure 6) and the barium data [*Guay and Falkner*, 1997; *Guay et al.*, 1999] suggests the following central Arctic Ocean circulation pattern: at the Mendeleyev Ridge and Chukchi Plateau the Eurasian river water mixed with North American river water, circulated across the Canada Basin (and perhaps into the Canadian Archipelago), passed over the Lomonosov Ridge, and was responsible for higher river runoff fractions in the western and central Amundsen Basin (in 1991) than were found in the eastern Amundsen Basin (in 1993 and 1995). For 1993, *Morison et al.* [1998] calculated a surface current of 0.02-0.03 m s^{-1} flowing along the Mendeleyev Ridge toward Greenland, adding support to the East Siberian Sea source area.

4.8. Pacific Water

The Pacific fraction, discussed in this context, is not a calculation with a salinity point of zero but rather is a fraction represented by the Pacific water salinity. The highest concentration of Pacific water, away from the Chukchi Sea shelf, is found between 75 and 100 m depth over the Chukchi Abyssal Plain (AOS94 stations 8, 10, and 11) with fractions of >50% of Pacific water fraction in the core of the 33.1 salinity water (Figure 7). A measurable Pacific water fraction in the 33.1 salinity water does not extend all the way to the Lomonosov Ridge in the AOS94 data; only the more buoyant (S < 33.1) surface portion of the Pacific inflow extends to the Lomonosov Ridge.

One Chukchi Sea shelf slope station, AOS94 station 6, has a lower Pacific water fraction near 33.1 salinity than do the adjacent stations, suggesting that the AOS94 section does not cross the shelf at the dominant location for UHW renewal. The high Pacific water fraction core at the Chukchi Abyssal Plain stations is associated with a $NO/PO_{(135)}$ signature of MECS. Therefore some of the Pacific inflow probably spreads toward the East Siberian Sea, renews the halocline near 33.1 salinity, flows off the shelf, and spreads toward the Chukchi Abyssal Plain. Herald Canyon is the closest submarine canyon to the Chukchi Abyssal Plain stations (Figure 1) and may guide the denser Pacific water to the Chukchi Abyssal Plain stations. *Weingartner et al.* [1998] analyzed 1991-1992 current meter and temperature and salinity mooring data and concluded that December and January, when open water areas had high heat loss, was the period of most dense water formation and fresh Bering Strait inflow was diverted through Hope Valley toward Herald Canyon.

The surface samples for the Pacific water percentage in Figure 7 can be compared with the Pacific water calculations of *Jones et al.* [1998] for the upper 30 m. The Pacific water percentage for surface samples depicted in Figure 7 are slightly lower than those of *Jones et al.* [1998] because the nitrate-phosphate method calculates the Atlantic water and Pacific water fractions but does not separate out the river runoff or sea ice meltwater fractions. These differences are small compared to the general similarity between these two different approaches that reconstruct a similar spatial distribution for the Pacific water mass.

The *Louis S. St-Laurent* crossed the Lomonosov Ridge in 1994 close to the stations *Oden* occupied in 1991 providing an opportunity to examine temporal changes in water properties at the same location. Near the Lomonosov Ridge, stations from both cruises are almost identical with respect to river runoff and sea ice fractions, but the AOS94 stations exhibit a significant decrease in Pacific water fraction and increase in Atlantic water fraction compared to the ARCTIC91 stations (Figure 8). ARCTIC91 station 23 contains more than 18% Pacific water near the surface compared to AOS94 station 30, which contains only 3-4% at the surface. This is equivalent to a decrease in Pacific water inventory from 9.2 m in 1991 to 1.6 m in 1994. Essentially, the 13 m Pacific water inventory isopleth shifted from directly over the Lomonosov Ridge in 1991 to the Mendeleyev Ridge in 1994 (Plate 1).

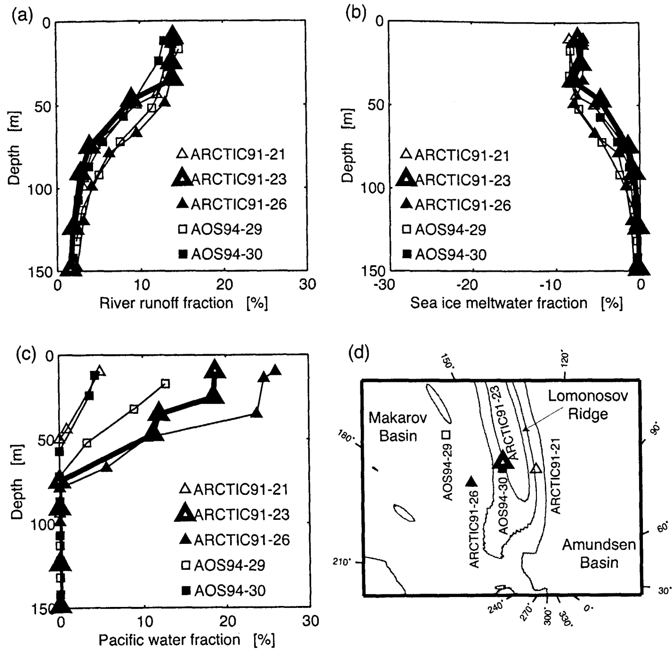

Figure 8. Comparison of 1991 and 1994 stations near the Lomonosov Ridge for (a) river runoff fraction, (b) sea ice meltwater fraction (positive = meltwater; negative = ice formation), (c) Pacific water fraction, and (d) location for these stations.

Historical data can be used to compare temporal changes in the distribution of the denser Pacific inflow that renews the halocline near 33.1 salinity. *Coachman and Barnes* [1961] defined this portion of the halocline as Winter Bering Sea Water. *Cooper et al.* [1997] define it as a winter ventilation signature. *Treshnikov* [1985] presents a silicate section for a location similar to that of the AOS94 section. The Treshnikov section starts at 71°N, 175°W, near Wrangel Island (near AOS94 station 2 at 72°08'N, 168°50'W) and ends at 89°N, 90°E, i.e., north of ARCTIC91 station 18 (88°11'N, 99°E). UHW has traditionally been associated with a nutrient maximum. Therefore variability in the extent of UHW can be determined by comparing silicate sections to the Treshnikov silicate section (Figure 9). The farthest northward extent of the 20 μmol kg^{-1} silicate maximum on the AOS94 section is to the southern edge of the Mendeleyev Ridge, whereas the 20 μmol L^{-1} silicate contour on the Treshnikov section extends across the Makarov Basin to the Lomonosov Ridge.

Silicate concentrations up to 40 μmol kg^{-1} were measured at T3 Ice station 703 in the Canada Basin near the center of the Alpha-Mendeleyev Ridge in 1969, over the Alpha Ridge from CESAR Ice station in 1983, and at the Lomonosov Ridge near the North Pole in 1979 from LOREX Ice station [*Kinney et al.*, 1970; *Moore et al.*, 1983; *Jones and Anderson*, 1986]. The T3 and CESAR stations are located closer to the Canadian shelf than the AOS94 stations and may lie along a path where the Pacific water circulates to Fram Strait. Other Canadian Basin data record the shifts in the Atlantic water and Pacific water front in the early 1990s. *McLaughlin et al.* [1996] and *Morison et al.* [1998] report data collected in 1993 that record the frontal position between Atlantic and Pacific water masses at the Alpha-Mendeleyev Ridge, and *Carmack et al.* [1997] also document this feature using data from 1994. The mass balance approach of this contribution has quantified these shifts, which now can be incorporated into models that test proposed forcing mechanisms.

4.9. Possible Causes for Observed Arctic Ocean Changes

Questions remain as to the causes for these observed changes in the Arctic Ocean basin, but mounting atmospheric and oceanographic evidence points to potential forcing mechanisms. Atmospheric pressure field shifts known as the Arctic Oscillation and the NAO achieved an extreme state for winter climatic forcing over the Arctic and Nordic Seas in the 1990s [*Dickson et al.*, 1996; *Walsh et al.*, 1996; *Thompson and Wallace*, 1998; *Dickson*, 1999]. The shift in atmospheric forcing is associated with a decrease in the extent of the Beaufort gyre, a shift to a cyclonic wind-forced circulation, and a decrease in the extent of Arctic sea ice [*Johannessen et al.*, 1995; *Serreze et al.*, 1995; *Maslanik et al.*, 1996; *Proshutinsky and Johnson*, 1997; *Levi*, 2000]. *Macdonald et al.* [1999] document a dramatic 4-6 m increase in sea ice melt in the Beaufort Sea after 1989 that coincides with a shift in the Arctic Oscillation index (i.e., a shift toward less anticyclonic wind forcing).

Amundsen Basin stations for a cruise in 1996 (ARK XII/1) just east of ARCTIC91 stations record a decrease in the river runoff inventories from 10 to 12 m in 1991 to 6 to 8 m in 1996 [*Ekwurzel*, 1998]. These temporal and spatially separated data sets lend support to *Steele and Boyd's* [1998] hypothesis for the retreat of the cold halocline layer they observed in 1995 from the Eurasian Basin as a shift in Siberian shelf river runoff outflow from the Amundsen Basin to the Makarov Basin. Thus dynamic atmospheric forcing may be reorganizing the mean freshwater circulation patterns enough to diminish the freshwater cap in the Amundsen Basin during the 1990s.

Björk [1990] used a one-dimensional circulation model for the upper 300 m of the Arctic Ocean and found that varying the Bering Strait inflow had a significant impact on the halocline nutrient profiles. Winter hydrographic surveys in the Beaufort Sea and southern Canada Basin, between 1979 and 1996 are a remarkable time series where Melling [1998] observed cooling (by 0.12°C at the 34.5 isohaline) of the lower halocline, a thickening of the Atlantic layer, and the warming and freshening of the water below the Atlantic water temperature maximum in the 1990s. *Melling* [1998] calls upon the weakening of the Siberian High to have caused a decrease in upper halocline renewal from the Pacific side.

Furthermore, *Carmack et al.* [1995, 1997], and *Swift et al.* [1997] propose that the warmer Atlantic water, found in the Makarov Basin in 1993 and 1994, may arise from warmer Atlantic inflow source waters in the Norwegian Sea. The most positive phase of the NAO in the late 1980s and early 1990s resulted in an increase in temperature of Atlantic water flowing north through Fram Strait to the highest recorded values [*Dickson*, 1999]. *Zhang et al.* [1998] present model results for the 1989-1996 time period of a 0.2 Sv increase of Atlantic water inflow through Fram Strait and a 0.5 Sv increase through the Barents Sea branch, which is balanced by a 0.7 Sv increase in outflow of Arctic water through Fram Strait. This leads to an increase of heat and salt in the Arctic Ocean and a decrease in ice volume. They propose that the increased penetration of Atlantic water into the Arctic Ocean is linked to a weakening of the Beaufort gyre and an increase in cyclonic systems that track into the Arctic from the North Atlantic. UHW distribution during the early 1990s has changed from that seen during surveys in the 1960s, 1970s, and 1980s. This change may be part of a shift

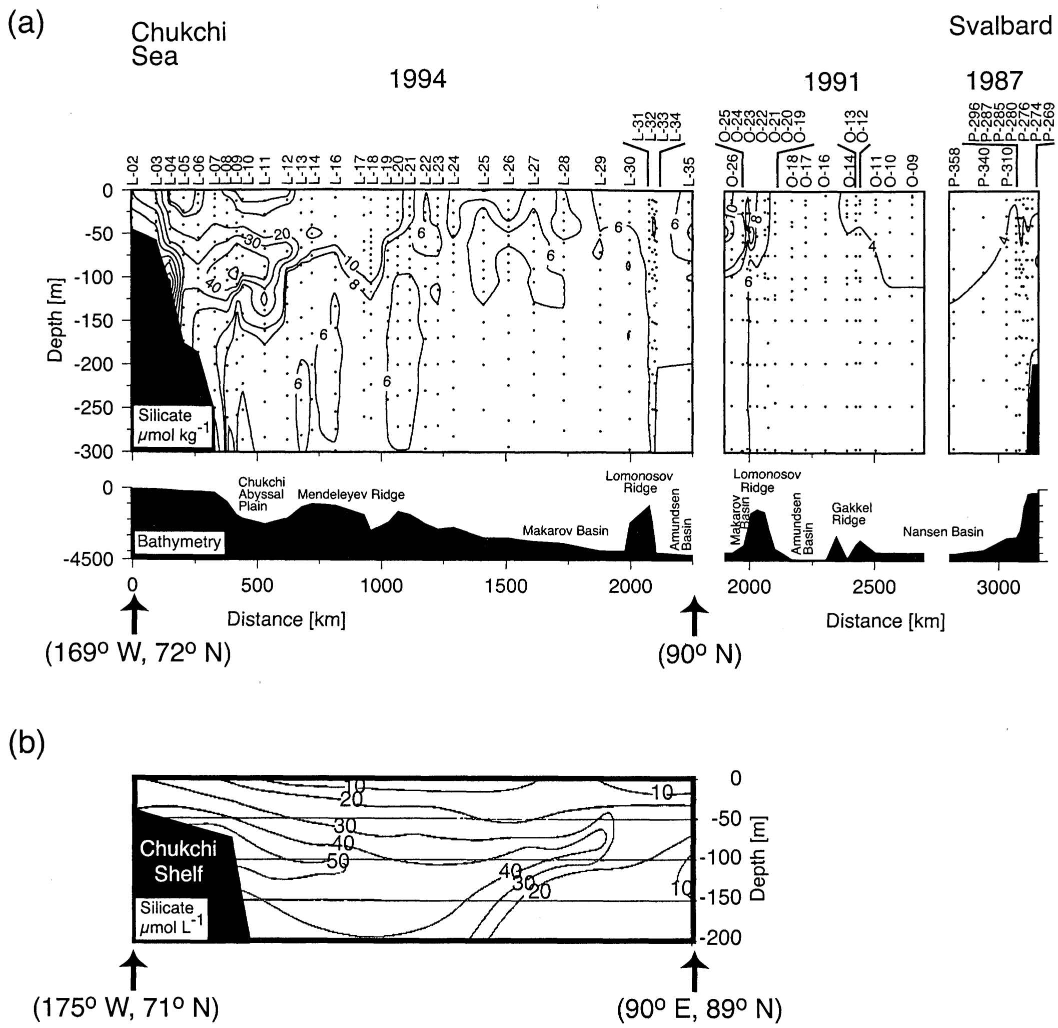

Figure 9. (a) Silicate (μmol kg^{-1}) sections following the format of Figure 7. Silicate data are from *Anderson et al.* [1989; 1994], and *Swift et al.* [1997]. (b) Silicate (μmol L^{-1}) section adapted from *Treshnikov* [1985].

between the balance of Atlantic and Pacific inflow strength in combination with the shifts in the atmospheric circulation.

4.10. Renewal of Halocline Waters

There are several ways to define the "age" of water. *Becker and Björk* [1996] define bulk residence time as the time it takes for the tracer content to be reduced by a factor of $1/e$. The ^{3}H-^{3}He age differs from this bulk residence time because the tracer age represents the mean transit time from the source region due to advection and mixing processes. *Becker and Björk* [1996] injected river water with age zero and a constant tritium concentration at each model level to produce an age distribution of the relative amount of each year's river runoff within each layer. The weighted mean age from the age distribution within each model level gives a similar age to the ARK IV/3 ^{3}H-^{3}He results used in their comparison.

As first observed in 1987 data [*Schlosser et al.*, 1990], the ARCTIC91 and AOS94 stations, with the exception of those from the southern Nansen Basin, have ^{3}H-^{3}He ages that increase gradually from the surface to the lower halocline (~34.2 salinity) and then increase dramatically to 34.5 salinity. This increase in age gradient is followed by a decrease in age gradient to the Atlantic water (Figure 10).

Rudels et al. [1996] suggest that the halocline waters, once formed, follow the Atlantic water circulation. The ^{3}H-^{3}He age profile represents the balance of waters renewing the densest part of the halocline combined with shear between the LHW (slow circulation) and the Atlantic water (relatively rapid circulation). *Cavalieri and Martin* [1994] calculate the total contribution of dense waters from Arctic coastal polynyas to the cold halocline to be 0.7-1.2 Sv. Presumably, a smaller portion of this total production renews the densest portion of the halocline each year. This is a much smaller rate when compared to the flow of Atlantic water estimated to be 1 Sv from the Fram Strait branch [*Rudels*, 1987] and 2 Sv from the Barents Sea branch [*Blindheim*, 1989].

LHW directly over the Gakkel Ridge and Lomonosov Ridge (~ 150 m) has higher ^{3}H-^{3}He ages than the waters on the flanks of each ridge (or in the case of the Gakkel Ridge, more central Nansen Basin and Amundsen Basin stations). Halocline age contours dome over the Gakkel Ridge and Lomonosov Ridge (Figure 10). Immediately below the halocline waters, over the Lomonosov Ridge, the trend of age contours reverses: relatively recently renewed water extends deeper to the ridge compared to relatively slow renewal of adjacent waters in the Makarov Basin. The highest ^{3}H-^{3}He ages are found over the Gakkel Ridge

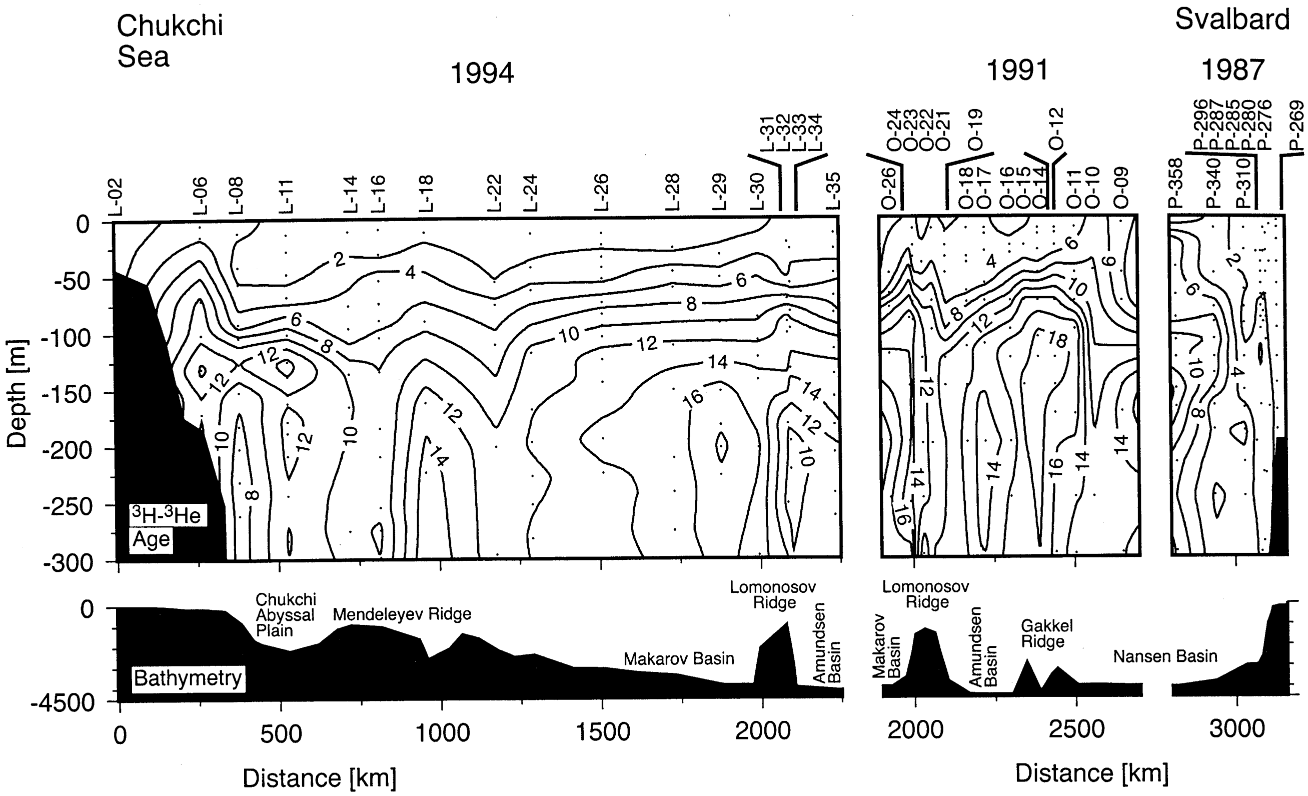

Figure 10. ^{3}H-^{3}He age sections follow the format of Figure 7.

(ARCTIC91 stations 11, 12, 14-16, 48, and 49) and the Makarov Basin adjacent to the Lomonosov Ridge (ARCTIC91 station 26). However, there is a narrow band of low tracer age water on the Eurasian Basin flanks of the Gakkel Ridge and the Lomonosov Ridge. This pattern implies a rapid cyclonic circulation around the Eurasian Basin perimeter in narrow boundary currents similar to the pattern described by *Rudels et al.* [1994].

LHW ages do not exhibit a monotonic ^{3}H-^{3}He age increase from the Eurasian Basin to the Canada Basin. The age distribution implies either that this portion of the LHW is frequently ventilated from local shelf sources or isopycnal mixing is quite rapid on the basin scale. The $NO/PO_{(135)}$ data from Chukchi Abyssal Plain LHW stations show mixing between Barents Sea and Chukchi Sea plus East Siberian Sea waters. Most LHW at Canadian Basin stations in this study retain the Barents Sea $NO/PO_{(135)}$ signature. This suggests that shelf renewal at this salinity is usually a minor addition in the Canadian Basin. Isopycnal mixing is quite rapid according to the tracer ages, with renewal from the shelf sources probably being a second-order effect.

UHW ^{3}H-^{3}He ages were remarkably uniform at 4.3 ± 1.7 years. However, there are slight differences that may be related to broad circulation patterns. Slightly younger ^{3}H-^{3}He ages (~2-5 years) over the Mendeleyev Ridge, compared to the adjacent Chukchi Abyssal Plain stations (~9 years), are further evidence for the juncture of the Mendeleyev Ridge and the East Siberian Sea as the main release point from the shelf for freshwater flow in 1994. Most of the Eurasian Basin waters in the 33.1 ± 0.3 salinity range do not exhibit the nutrient peak and do not contain Pacific-derived UHW. The stations that do have determinable Pacific water fractions demonstrate a slight increase in ^{3}H-^{3}He age from the Lomonosov Ridge (~ 3-4 years) to the Morris Jesup Plateau (~8 years).

The mean ^{3}H-^{3}He age measured for the 34.2 ± 0.2 salinity surface is 9.6 ± 4.6 years. Despite the weakness of the central Arctic Ocean mean flow field, properties could be transported rapidly across the basin by eddies [*Manley and Hunkins*, 1985; *Aagaard and Carmack*, 1994]. A high-resolution model forced with 1992 winds calculated (1) increased annual mean velocities within 0-45 m at the shelf slope perimeter throughout most of the Arctic Ocean, the Barents Sea shelf, Chukchi Plateau, and the Alpha-Mendeleyev Ridge and (2) high surface eddy kinetic energy in the Canada Basin, especially near the Chukchi Plateau (W. Maslowski, personal communication, 1998). The ^{3}H-^{3}He age results support the notion that boundary currents carry the major properties along the Arctic Ocean perimeter (Atlantic water inflow and shelf renewal) and the eddies rapidly transport these properties into the interior. Similar trends have been observed in the Canada Basin [*Smethie et al.,* 2000].

5. Conclusions

The salinity, nutrient, dissolved oxygen, $\delta^{18}O$, tritium, and helium data collected in the early 1990s extend our insight into the possible circulation patterns within the Arctic Ocean. AOS94 stations did not sample the Beaufort Gyre but instead were situated close to the East Siberian Sea and captured evidence for an UHW renewal location (East Siberian Sea close to the Chukchi Abyssal Plain). These tracer data also establish the Mendeleyev Ridge as the main area for river runoff (a mixture of freshwater from Barents Sea, Kara Sea, Laptev Sea, and East Siberian Sea) to flow off the shelf in 1994. This freshwater mixes with freshwater from the Canadian rivers and circulates through the Canadian Basin back over the Lomonosov Ridge. It forms a freshwater cap within the western Amundsen Basin and north of Greenland.

PO_4* is an effective tracer, in combination with $\delta^{18}O$ and salinity, for calculating the Pacific water fraction of surface and halocline waters. The balance between Pacific and Atlantic water fractions changed between 1991 and 1994 over the Lomonosov Ridge, signaling the retreat of the Pacific water front from the Lomonosov to the Mendeleyev Ridge. It remains to be seen if this shift is temporary or long term. Dramatic changes began to occur in the convective regions of the north Atlantic such as the Greenland Sea in the 1980s [*Schlosser et al.*, 199; *Bönisch et al.*, 1997] and now dramatic shifts are occurring between water masses in the Arctic Ocean in the 1990s. Evidence suggests that changes in atmospheric forcing regimes collectively known as the Arctic Oscillation and NAO may be driving the reorganization of freshwater masses in the Arctic Ocean.

Acknowledgments. This research relied on the generous support of the chief scientists, officers, and crew of the FS *Polarstern*, IB *Oden*, and CCGS *Louis S. St-Laurent*. Numerous individuals from the Alfred Wegener Institute for Polar and Marine Research (Germany), Bedford Institute of Oceanography (Canada), Institute of Ocean Sciences (Canada), Scripps Institution of Oceanography (United States), and University of Göteborg (Sweden) provided high-quality hydrographic and nutrient data. Measurement of the unpublished portion of the tritium, helium, and ^{18}O data analyzed in this study benefited from the assistance of N. Asif, G. Bönisch, D. Breger, D. Darro, S. Hellman, S. Khatiwala, L. Kohandoust, A. Ludin, G. Mandal, M. K. Mendelson, M. Peacock, R. Weppernig, D. Smith, and F. Zaucker. We thank Rob Macdonald for sharing his sea ice phosphate measurements from the Beaufort Sea, and Hajo Eicken for his insights regarding $\delta^{18}O$ fractionation in sea ice. The sections and maps were produced using GMT [*Wessel and Smith*, 1995]. The invaluable assistance of Vicki Childers much improved the GMT section and map figures. Critical reviews on early drafts by Stephanie Pfirman, James Simpson, and William Smethie Jr. are much appreciated. Anonymous reviewers provided valuable suggestions for improving the manuscript. The W. M. Keck Foundation provided the funds for the helium isotope mass spectrometers used to measure the helium samples analyzed in this study. Financial support was provided by the Office of Naval Research (grants N0014-90-J-1362, N00014-94-1-0809, and N00014-93-1-0830) and the National Science Foundation (grant DPP 90-22890). LDEO contribution 6098.

References

Aagaard, K., and E.C. Carmack, The role of sea ice and other fresh water in the Arctic circulation, *J. Geophys. Res.*, *94*, 14,485-14,498, 1989.

Aagaard, K., and E.C. Carmack, The Arctic Ocean and climate: A perspective, in *The Polar Oceans and Their Role in Shaping the Global Environment*, Geophys. Mongr. Ser. vol. 85, edited by O.M. Johannessen, R.D. Muench, and J.E. Overland, pp. 5–20, AGU, Washington, D.C., 1994.

Aagaard, K., L.K. Coachman, and E. Carmack, On the halocline of the Arctic Ocean, *Deep Sea Res.*, *Part A*, *28*, 529-545, 1981.

Aagaard, K., J.H. Swift, and E.C. Carmack, Thermohaline circulation in the Arctic Mediterranean seas, *J. Geophys. Res.*, *90*, 4833-4846, 1985.

Anderson, L., and J. Sarmiento, Redfield ratios of remineralization determined by nutrient data analysis, *Global Biogeochem. Cycles*, *8*, 65-80, 1994.

Anderson, L.G., Chemical oceanography of the Arctic and its shelf seas, in *Arctic Oceanography: Marginal Ice Zones and Continental Shelves*, Coastal Estuarine Stud. vol. 49, edited by W.O. Smith Jr. and J.M. Grebmeier, pp. 183-202, AGU, Washington, DC, 1995.

Anderson, L.G., and E.P. Jones, Transport of CO2 into Arctic and Antarctic seas: Similarities and differences in driving processes, *J. Mar. Syst.*, *1*, 81-95, 1991.

Anderson, L.G., E.P. Jones, R. Lindegren, B. Rudels, and P.I. Sehlstedt, Nutrient regeneration in cold, high salinity bottom water of the Arctic shelves, *Cont. Shelf Res.*, *8*, 1345-1355, 1988.

Anderson, L.G., E.P. Jones, K.P. Koltermann, P. Schlosser, J.H. Swift, and D.W. Wallace, The first oceanographic section across the Nansen Basin in the Arctic Ocean, *Deep Sea Res.*, *Part A*, *36*, 475-482, 1989.

Anderson, L.G., G. Björk, O. Holby, E.P. Jones, G. Kattner, K.P. Koltermann, B. Liljeblad, R. Lindegren, B. Rudels, and J. Swift, Water masses and circulation in the Eurasian Basin: Results from the Oden 91 expedition, *J. Geophys. Res.*, *99*, 3273–3283, 1994.

Bauch, D., The distribution of $\delta^{18}O$ in the Arctic Ocean: Implications for the freshwater balance of the halocline and the sources of deep and bottom waters, Rep. *159,* 144 pp., Alfred Wegener Inst. for Polar and Mar. Res., Bremerhaven, Germany, 1995.

Bauch, D., P. Schlosser, and R.G. Fairbanks, Freshwater balance and the sources of deep and bottom waters in the Arctic Ocean inferred from the distribution of $H_2{}^{18}O$, *Prog. Oceanogr.*, *35*, 53-80, 1995.

Bayer, R., P. Schlosser, G. Bönisch, H. Rupp, F. Zaucker, and G. Zimmek, Performance and blank components of a mass spectrometric system for routine measurement of helium isotopes and tritium by the ^{3}He ingrowth method., Sitzungsber. *5* Heidelberger Akad. der Wissenschaften Mathematisch-Naturwissenschaftliche Klasse, Berlin, Germany 1989.

Becker, P., The effect of Arctic river hydrological cycles on Arctic Ocean circulation, Ph.D. thesis, Old Dominion Univ., Norfolk, Va., 1995.

Becker, P., and G. Björk, Residence times in the upper Arctic Ocean, *J. Geophys. Res.*, *101*, 28,377-28,396, 1996.

Björk, G., The vertical distribution of nutrients and oxygen 18 in the upper Arctic Ocean, *J. Geophys. Res.*, *95*, 16,025-16,036, 1990.

Blindheim, J., Cascading of Barents Sea bottom water into the Norwegian Sea, *Rapp. P. V. Reun. Cons. Int. Explor. Mer.*, *188*, 49-58, 1989.

Blindheim, J., V. Borovkov, B. Hansen, S.-A. Malmberg, W.R. Turrell, and S. Østerhus, Upper layer cooling and freshening in the Norwegian Sea in relation to atmospheric forcing, *Deep Sea Res.*, *Part A*, *47*, 655-680, 2000.

Bönisch, G., J. Blindheim, J.L. Bullister, P. Schlosser, and D.W.R. Wallace, Long-term trends of temperature, salinity, density, and transient tracers in the central Greenland Sea, *J. Geophys. Res.*, *102*, 18,553-18,571, 1997.

Broecker, W.S., "NO," A conservative-mass tracer, *Earth Planet. Sci. Lett.*, *23*, 100-107, 1974.

Broecker, W.S., T. Takahashi, and T. Takahashi, Sources and flow patterns of deep-ocean waters as deduced from potential temperature, salinity, and initial phosphate concentration, *J. Geophys. Res.*, *90*, 6925-6939, 1985.

Broecker, W.S., S. Sutherland, W. Smethie, T.H. Peng, and G. Östlund, Oceanic radiocarbon: Separation of the natural and bomb components, *Global Biogeochem. Cycles*, *9*, 263-288, 1995.

Broecker, W.S., S.L. Peacock, S. Walker, R. Weiss, E. Fahrbach, M. Schroeder, U. Mikolajewicz, C. Heinze, R. Key, T.-H. Peng, and S. Rubin, How much deep water is formed in the Southern Ocean?, *J. Geophys. Res.*, *103*, 15,833-15,843, 1998.

Carmack, E.C., Large-scale physical oceanography of polar oceans, in *Polar Oceanography,* part A, *Physical Science*, edited by W.O. Smith Jr., pp. 171-222, Academic, San Diego, California, 1990.

Carmack, E.C., R.W. Macdonald, R.G. Perkin, F.A. McLaughlin, and R.J. Pearson, Evidence for warming of Atlantic water in the southern Canadian Basin of the Arctic Ocean: Results from the Larsen-93 expedition, *Geophys. Res. Lett.*, *22*, 1061-1064, 1995.

Carmack, E.C., K. Aagaard, J.H. Swift, R.W. Macdonald, F.A. Mclaughlin, E.P. Jones, R.G. Perkin, J.N. Smith, K.M. Ellis, and L.R. Killius, Changes in temperature and tracer distributions within the Arctic Ocean: Results from the 1994 Arctic Ocean section, *Deep Sea Res. Part B*, *44*, 1487-1502, 1997.

Cavalieri, D.J., and S. Martin, The contribution of Alaskan, Siberian, and Canadian coastal polynyas to the cold halocline layer of the Arctic Ocean, *J. Geophys. Res.*, *99*, 18,343-18,362, 1994.

Clarke, W.B., W.B. Jenkins, and Z. Top, Determination of tritium by mass spectrometric measurement of ^{3}He, *Int. Appl. Radiat. Isot.*, *27*, 515-527, 1976.

Coachman, L.K., and C.A. Barnes, The contribution of Bering Sea water to the Arctic Ocean, *Arctic*, *14*, 147-161, 1961.

Coachman, L.K., and C.A. Barnes, Surface water in the Eurasian Basin of the Arctic Ocean, *Arctic*, *15*, 251-277, 1962.

Coachman, L.K., K. Aagaard, and R.B. Tripp, *Bering Strait: The Regional Physical Oceanography*, 172 pp., Univ. of Wash. Press, Seattle, 1975.

Codispoti, L.A., and F.A. Richards, Micronutrient distributions in the East Siberian and Laptev seas during summer 1963, *Arctic*, *21*, 67-83, 1968.

Cooper, L.W., T.E. Whitledge, J.M. Grebmeier, and T. Weingartner, The nutrient, salinity, and stable oxygen isotope composition of Bering and Chukchi Seas waters in and near the Bering Strait, *J. Geophys. Res.*, *102*, 12,563-12,573, 1997.

Craig, H., Standard for reporting concentrations of deuterium and oxygen-18 in natural waters, *Science*, *133*, 1833-1844, 1961.

Craig, H., and B. Hom, Relationships of deuterium, oxygen 18, and chlorinity in the formation of sea ice, *Eos Trans. AGU*, *49*, 216-217, 1968.

Dickson, B., All change in the Arctic, *Nature*, *397*, 389-390, 1999.

Dickson, R.R.J., J. Meincke, S.-A. Malmberg, and A.J. Lee, The "great salinity anomaly" in the northern North Atlantic 1968–1982, *Prog. Oceanogr.*, *20*, 103–151, 1988.

Dickson, R., J. Lazier, J. Meincke, P. Rhines, and J. Swift, Long-term coordinated changes in the convective activity of the North Atlantic, *Prog. Oceanogr.*, *38*, 241-295, 1996.

Eicken, H., Deriving modes and rates of ice growth in the Weddell Sea from microstructural, salinity and stable-isotope data, in *Antarctic sea ice: Physical Processes, Interactions and Variability*, *Antarctic Res. Ser.*, vol. 74, edited by M. O. Jeffries, pp. 89-122, AGU, Washington, D.C., 1998.

Ekwurzel, B., Circulation and mean residence times in the Arctic Ocean derived from tritium, helium, and oxygen-18 tracers, Ph.D. thesis, Columbia Univ., New York, 1998.

Epstein, S., and T. Mayeda, Variation of oxygen-18 content of waters from natural sources, *Geochem. Cosmochim. Acta*, *4*, 213-224, 1953.

Fairbanks, R.G., The origin of continental shelf and slope water in the New York Bight and Gulf of Maine: Evidence from $H_2{}^{18}O/H_2{}^{16}O$ ratio measurements, *J. Geophys. Res.*, *87*, 5796-5808, 1982.

Frank, M., Spurenstoffuntersuchungen zur zirkulation im Eurasischen Becken des Nordpolarmeeres, Ph.D. thesis, Ruprecht Karls Univ. Heidelberg, Heidelberg, Germany, 1996.

Gonfiantini, R., The δ-notation and the mass-spectrometric measurement techniques, in *Stable Isotope Hydrology: Deuterium and Oxygen-18 in the Water Cycle*, edited by J.R. Gat and R. Gonfiantini, pp. 35-84, Int. At. Energy Agency, Vienna, 1981.

Gordeev, V.V., J.M. Martin, I.S. Sidorov, and M.V. Sidorova, A reassessment of the Eurasian river input of water, sediment, major elements, and nutrients to the Arctic Ocean, *Am. J. Sci.*, *296*, 664-691, 1996.

Grebmeier, J.M., L.W. Cooper, and M.J. DeNiro, Oxygen isotopic composition of bottom seawater and tunicate cellulose used as indicators of water masses in the northern Bering and Chukchi Seas, *Limnol. Oceanogr.*, *35*, 1182-1195, 1990.

Guay, C.K., and K.K. Falkner, Barium as a tracer of Arctic halocline and river waters, *Deep Sea Res., Part B*, *44* (8), 1543-1569, 1997.

Guay, C.K., G.P. Klinkhammer, K.K. Falkner, R. Benner, P.G. Coble, T.E. Whitledge, B. Black, F.J. Bussell, and T.A. Wagner, High-resolution measurements of dissolved organic carbon in the Arctic Ocean by in situ fiber-optic spectrometry, *Geophys. Res. Lett.*, *26*, 1007-1010, 1999.

Häkkinen, S., An Arctic source for the Great Salinity Anomaly: A simulation of the Arctic ice-ocean system for 1955-1975, *J. Geophys. Res.*, *98*, 16,397-16,410, 1993.

Johannessen, O.M., M. Miles, and E. Bjorgo, The Arctic's shrinking sea ice, *Nature*, *376*, 126-127, 1995.

Jones, E.P., and L.G. Anderson, On the origin of the chemical properties of the Arctic Ocean halocline, *J. Geophys. Res.*, *91*, 10,759-10,767, 1986.

Jones, E.P., L.G. Anderson, and J.H. Swift, Distribution of Atlantic and Pacific waters in the upper Arctic Ocean: Implications for circulation, *Geophys. Res. Lett.*, *25*, 765-768, 1998.

Kinney, D.J., M.E. Arhelger, and D.C. Burrell, Chemical characteristics of the water masses in the Amerasian Basin of the Arctic Ocean, *J. Geophys. Res.*, *75*, 4097-4104, 1970.

Kipphut, G.W., Glacial meltwater input to the Alaska Coastal Current: Evidence from oxygen isotope measurements, *J. Geophys. Res.*, *95* (C4), 5177-5181, 1990.

Lehmann, M., and U. Siegenthaler, Equilibrium oxygen and hydrogen isotope fractionation between ice and water, *J. Glaciol.*, *37*, 23-26, 1991.

Létolle, R., J.M. Martin, A.J. Thomas, V.V. Gordeev, S. Gusarova, and I.S. Sidorov, ^{18}O abundance and dissolved silicate in the Lena delta and Laptev Sea (Russia), *Mar. Chem.*, *43*, 47-64, 1993.

Levi, B.G., The decreasing Arctic ice cover, *Phys. Today*, *53*, 19-20, 2000.

Ludin, A., R. Weppernig, G. Bönisch, and P. Schlosser, Mass spectrometric measurement of helium isotopes and tritium, *L-DEO Tech. Rep. 98-6*, 42 pp., Lamont-Doherty Earth Obs., Palisades, New York, 1998.

Macdonald, R.W., and E.C. Carmack, The role of large-scale under-ice topography in separating estuary and ocean on an Arctic shelf, *Atmos. Ocean*, *29*, 37-53, 1991.

Macdonald, R.W., C.S. Wong, and P.E. Erickson, The distribution of nutrients in the southeastern Beaufort Sea: Implications for water circulation and primary production, *J. Geophys. Res.*, *92*, 2939-2952, 1987.

Macdonald, R.W., E.C. Carmack, F.A. McLaughlin, K. Iseki, D.M. Macdonald, and M.C. O'Brien, Composition and modification of water masses in the Mackenzie shelf estuary, *J. Geophys. Res.*, *94*, 18,057-18,070, 1989.

Macdonald, R.W., D.W. Paton, E.C. Carmack, and A. Omstedt, The freshwater budget and under-ice spreading of the Mackenzie River water in the Canadian Beaufort Sea based on salinity and $^{18}O/^{16}O$ measurements in water and ice, *J. Geophys. Res.*, *100*, 895-919, 1995.

Macdonald, R.W., E.C. Carmack, F.A. McLaughlin, K.K. Falkner, and J.H. Swift, Connections among ice, runoff and atmospheric forcing in the Beaufort Gyre, *Geophys. Res. Lett.*, *26*, 2223-2226, 1999.

Makkaveev, P.N., and P.A. Stunzhas, Hydrochemical characteristics of the Kara Sea, *Oceanology, Engl. Transl.*, *34*, 600-605, 1995.

Manley, T.O., and K. Hunkins, Meso-scale eddies of the Arctic Ocean, *J. Geophys. Res.*, *90*, 4911-4930, 1985.

Maslanik, J.A., M.C. Serreze, and R.G. Barry, Recent decreases in Arctic summer ice cover and linkages to atmospheric circulation anomalies, *Geophys. Res. Lett.*, *23*, 1677-1680, 1996.

McLaughlin, F.A., E.C. Carmack, and R.W. Macdonald, Physical and geochemical properties across the Atlantic/Pacific water mass front in the southern Canadian Basin, *J. Geophys. Res.*, *101*, 1183-1197, 1996.

Melling, H., Hydrographic changes in the Canada Basin of the Arctic Ocean, 1979-1996, *J. Geophys. Res.*, *103*, 7637-7645, 1998.

Melling, H., and R.M. Moore, Modification of halocline source waters during freezing on the Beaufort Sea shelf: evidence from oxygen isotopes and dissolved nutrients, *Cont. Shelf Res.*, *15*, 89-113, 1995.

Melnikov, I.A., *The Arctic Sea Ice Ecosystem*, 204 pp., Gordon and Breach, Newark, N.J., 1997.

Moore, R.M., M.G. Lowings, and F.C. Tan, Geochemical profiles in the central Arctic Ocean: Their relation to freezing and shallow circulation, *J. Geophys. Res.*, *88*, 2667-2674, 1983.

Morison, J., M. Steele, and R. Andersen, Hydrography of the upper Arctic Ocean measured from the nuclear submarine U.S.S. Pargo, *Deep Sea Res. Part A*, *45*, 15-38, 1998.

Olsson, K., Dissolved carbon in the Arctic Ocean, Ph.D. thesis, Göteborg Univ., Göteborg, Sweden, 1997.

Östlund, H.G., and G. Hut, Arctic Ocean water mass balance from isotope data, *J. Geophys. Res.*, *89*, 6373-6381, 1984.

Pavlov, V.K., L.A. Timokhov, G.A. Baskakov, M.Y. Kulakov, V.K. Kurazhov, P.V. Pavlov, S.V. Pivovarov, and V.V. Stanovoy, Hydrometeorological regime of the Kara, Laptev, and East-Siberian Seas, *APL-UW TM1-96*, Appl. Phys. Lab. Univ. of Wash., Seattle, 1996.

Pfirman, S., M.A. Lange, I. Wollenberg, and P. Schlosser, Sea ice characteristics and the role of sediment inclusions in deep-sea deposition: Arctic-Antarctic comparisons, in *Geological History of the Polar Oceans: Arctic Versus Antarctic*, edited by U. Bleil and J. Thiede, pp. 187-211, Kluwer Acad., Norwell, Mass., 1990.

Pfirman, S.L., D. Bauch, and T. Gammelsrød, The Northern Barents Sea: Water mass distribution and modification, in *The Polar Oceans and Their Role in Shaping the Global Environment, Geophys. Monogr. Ser.*, vol. 85, edited by O.M. Johannessen, R.D. Muench, and J.E. Overland, pp. 77-94, AGU, Washington, D.C., 1994.

Pfirman, S.L., R. Colony, D. Nürnberg, H. Eicken, and I. Rigor, Reconstructing the origin and trajectory of drifting Arctic sea ice, *J. Geophys. Res.*, *102*, 12,575-12,586, 1997.

Proshutinsky, A.Y., and M.A. Johnson, Two circulation regimes of the wind-driven Arctic Ocean, *J. Geophys. Res.*, *102*, 12,493-12,514, 1997.

Rey, F., and H. Loeng, The influence of ice and hydrographic conditions on the development of phytoplankton in the Barents Sea, in *Marine Biology of Polar Regions and Effects of Stress on Marine Organisms*, edited by J.S. Gray and M.E. Christiansen, pp. 49-63, John Wiley, New York, 1985.

Roach, A.T., K. Aagaard, C.H. Pease, S.A. Salo, T. Weingartner, V. Pavlov, and M. Kulakov, Direct measurement of transport and water properties through the Bering Strait, *J. Geophys. Res.*, *100*, 18,443-18,457, 1995.

Roether, W., Water-CO_2 exchange set-up for the routine [18]oxygen assay of natural waters, *Int. J. Appl. Radiat. Isot.*, *321*, 379-387, 1970.

Rudels, B., On the Mass Balance of the Polar Ocean, With Special Emphasis on Fram Strait, Rep. 188, 53pp., Norsk Polarinst., Oslo, Norway, 1987.

Rudels, B., E.P. Jones, L.G. Anderson, and G. Kattner, On the intermediate depth waters of the Arctic Ocean, in *The Polar Oceans and Their Role in Shaping the Global Environment, Geophys. Mongr. Ser.*, vol. 85, edited by O.M. Johannessen, R.D. Muench, and J.E. Overland, pp. 33-46, AGU, Washington, D.C., 1994.

Rudels, B., L.G. Anderson, and E.P. Jones, Formation and evolution of the surface mixed layer and halocline of the Arctic Ocean, *J. Geophys. Res.*, *101*, 8807-8821, 1996.

Salmon, D.K., and C.P. McRoy, Nutrient-based tracers in the western Arctic: A new Lower Halocline Water defined, in *The Polar Oceans and Their Role in Shaping the Global Environment, Geophys. Mongr. Ser.*, vol. 85, edited by O.M. Johannessen, R.D. Muench, and J.E. Overland, pp. 47-61, AGU, Washington, D.C., 1994.

Schauer, U., R.D. Muench, B. Rudels, and L. Timokhov, Impact of eastern Arctic shelf waters on the Nansen Basin intermediate layers, *J. Geophys. Res.*, *102*, 3371-3382, 1997.

Schlosser, P., G. Bönisch, B. Kromer, K.O. Münnich, and K.P. Koltermann, Ventilation rates of the waters in the Nansen Basin of the Arctic Ocean derived from a multitracer approach, *J. Geophys. Res.*, *95*, 3265-3272, 1990.

Schlosser, P., G. Bönisch, M. Rhein, and R. Bayer, Reduction of deepwater formation in the Greenland Sea during the 1980s: Evidence from tracer data, *Science*, *251*, 1054-1056, 1991.

Schlosser, P., D. Bauch, R. Fairbanks, and G. Bönisch, Arctic river-runoff: Mean residence time on the shelves and in the halocline, *Deep Sea Res., Part A*, *41*, 1053-1068, 1994.

Schlosser, P., J.H. Swift, D. Lewis, and S.L. Pfirman, The role of the large-scale Arctic Ocean circulation in the transport of contaminants, *Deep Sea Res., Part B*, *42*, 1341-1367, 1995.

Serreze, M.C., J.A. Maslanik, J.R. Key, and R.F. Kokaly, Diagnosis of the record minimum in Arctic sea ice area during 1990 and associated snow cover extremes, *Geophys. Res. Lett.*, *22*, 2183-2186, 1995.

Smethie, W. M., Jr., P. Schlosser, G. Bönisch, and T. S. Hopkins, Renewal and circulation of intermediate waters in the Canadian Basin observed on the SCICEX 96 cruise, *J. Geophys. Res.*, *105*, 1105-1121, 2000.

Steele, M, and T. Boyd, Retreat of the cold halocline layer in the Arctic Ocean, *J. Geophys. Res.*, *103*, 10,419-10,435, 1998.

Steele, M., J.H. Morison, and T.B. Curtin, Halocline water formation in the Barents Sea, *J. Geophys. Res.*, *100*, 881-894, 1995.

Swift, J.H., and K. Aagaard, Seasonal transitions and water mass formation in the Iceland and Greenland Seas, *Deep Sea Res. part A*, *28*, 1107-1129, 1981.

Swift, J.H., E.P. Jones, K. Aagaard, E.C. Carmack, M. Hingston, R.W. Macdonald, F.A. McLaughlin, and R.G. Perkin, Waters of the Makarov and Canada Basins, *Deep Sea Res., Part II*, *44*, 1503-1529, 1997.

Takahashi, T., W.S. Broecker, and S. Langer, Redfield ratio based on chemical data from isopycnal surfaces, *J. Geophys. Res.*, *90*, 6907-6924, 1985.

Thompson, D.W.J., and J.M. Wallace, The Arctic Oscillation signature in the wintertime geopotential height and temperature fields, *Geophys. Res. Lett.*, *25*, 1297-1300, 1998.

Thorndike, A.S., and R. Colony, Sea ice motion in response to geostrophic winds, *J. Geophys. Res.*, *87*, 5845-5852, 1982.

Treshnikov, A.F., *Arctic Atlas*, 204 pp., Nauchno Issled. Inst., Moscow, 1985.

Untersteiner, N., Natural desalination and equilibrium salinity profile of perennial sea ice, *J. Geophys. Res.*, *73*, 1251–1257, 1968.

Unterweger, M.P., B.M. Coursey, F.J. Schima, and W.B. Mann, Preparation and calibration of the 1978 National Bureau of Standards tritiated-water standards, *Int. J. Appl. Radiat. Isot.*, *31*, 611-614, 1980.

Walsh, J.E., W.L. Chapman, and T.L. Shy, Recent decrease of sea level pressure in the central Arctic, *J. Clim.*, *9*, 480-486, 1996.

Weingartner, T.J., D. Cavalieri, K. Aagaard, and Y. Sasaki, Circulation, dense water formation, and outflow on the northeast Chukchi shelf, *J. Geophys. Res.*, *103*, 7647-7661, 1998.

Wessel, P., and W.H.F. Smith, New version of the Generic Mapping Tools released, *Eos Trans. AGU*, *76*, 329, 1995.

Wilson, C., and D.W.R. Wallace, Using the nutrient ratio NO/PO as a tracer of continental shelf waters in the central Arctic Ocean, *J. Geophys. Res.*, *95*, 22,193-22,208, 1990.

Zhang, J., D.A. Rothrock, and M. Steele, Warming of the Arctic Ocean by a strengthened Atlantic inflow: Model results, *Geophys. Res. Lett.*, *25*, 1745-1748, 1998.

B. Ekwurzel, Department of Hydrology and Water Resources, The University of Arizona, J. W. Harshbarger Bldg., Tucson, AZ, 85721-0011, (e-mail: ekwurzel@hwr.arizona.edu).

R. G. Fairbanks, R. A. Mortlock, and P. Schlosser, Lamont-Doherty Earth Observatory of Columbia University, Palisades, NY 10964, (e-mail: fairbank@ldeo.columbia.edu, mortlock@ldeo.columbia.edu, peters@ldeo.columbia.edu).

J. H. Swift, Scripps Institution of Oceanography, University of California, San Diego, Mail Code 0214, Gilman Dr., La Jolla, CA 92093-0214, (e-mail: jswift@ucsd.edu).

(Received July 14, 1999; revised September 11, 2000;
accepted November 7, 2000.)